**Title**
STRUCTURE, STRENGTH, AND TOUGHNESS OF Fe/Cr/C MARTENSITIC STEELS



**Author**
McMahon, John A.

**Publication Date**
1973

LBL-1181

c.1

# STRUCTURE, STRENGTH, AND TOUGHNESS OF Fe/Cr/C MARTENSITIC STEELS

John A. McMahon

(M. S. Thesis)

January 1973

Prepared for the U. S. Atomic Energy Commission
under Contract W-740t-ENG-48



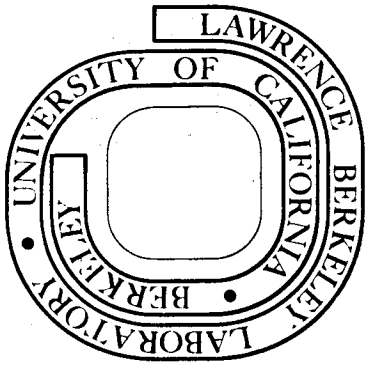


LBL-1181

c.1

25

## DISCLAIMER

Table of Contents

# STRUCTURE, STRENGTH, AND TOUGHNESS OF Fe/Cr/C MARTENSITIC STEELS

John A. McMahon

Inorganic Materials Research Division, Lawrence Berkeley Laboratory and Department of Materials Science and Engineering, College of Engineering; University of California, Berkeley, California

## ABSTRACT

The changes in microstructure and mechanical properties of Fe/Cr/C martensitic steels as functions of chromium and carbon content were investigated using transmission electron microscopy and tensile, compressive, and fracture toughness testing. The as-quenched martensitic microstructures and the carbide morphologies produced by tempering at 200, 400, and 600°C were analyzed. For a given carbon content, the volume fraction of martensite containing transformation twins increased with chromium concentration, demonstrating that chromium induces transformation twinning in martensite. $M_s$ temperature measurements showed that increasing the chromium level also lowers the $M_s$ temperature, and as expected the amount of autotempering during quenching decreased.

The common type of carbide morphology was observed in the tempered specimens. At 200°C a Widmanstatten pattern of $Fe_3C$ was found in the dislocated laths, while the twinned plates contained carbides along the twin boundaries and epsilon carbide in the adjacent matrix. Epsilon carbide was not observed in any other morphology or at any higher tempering temperature. At 400°C, interlath carbides formed, in addition to the

Widmanstatten and twin boundary carbides. Tempering at 600°C led to coarsening and spheroidization of the carbides and some recovery of the dislocation substructures. At each increase in tempering temperature, there appeared to be a reduction in the transformation twin density.

The electron microscopy also revealed thin sheets of retained austenite surrounding the martensite laths. The amount of retained austenite decreased as tempering temperature increased.

The mechanical properties of the as-quenched and tempered structures were investigated using tensile, compressive, and fracture toughness tests. These properties were then correlated with the martensitic substructures and carbide morphologies. It was found that for the same carbon level, an increase in the amount of transformation twinning due to a higher chromium concentration has a dramatic and deleterious effect on the fracture toughness of the as-quenched steels. In the two steels containing 0.35 wt.% C, raising the chromium content from 4 wt.% to 12 wt.% caused the percentage of twinned martensite to increase by almost a factor of two (as estimated from electron micrographs), and the plane strain fracture toughness to drop from 70 to 20 KSI-in.$^{1/2}$ The high chromium alloy also had a higher yield strength: 300 KSI vs 240 KSI for the low chromium alloy. This indicates that an increase in twin density acts as a major strengthening and embrittling mechanism. However, when tempered to equivalent yield strengths, the 12 wt.% Cr with the higher twin density continued to have much poorer fracture toughness compared to the 4 wt.% Cr alloy with a lower twin density. Thus it has been established that in Fe/Cr/C steels with the carbon content held constant, there is a direct correlation between transformation twinning and strength and toughness.

One of the results of this systematic study of the microstructure and mechanical properties of Fe/Cr/C martensitic steels has been the discovery of a new alloy with mechanical properties equivalent to those of 18 Ni maraging steels which could be produced at a significantly lower cost.

# I. INTRODUCTION

During the past decade, applications of transmission electron microscopy and fracture toughness testing have contributed significantly to our understanding of the factors controlling the properties of martensitic structural steels. The electron microscope permits a detailed, quantitative study of substructure, while fracture toughness testing provides a more specific and useful measure of toughness than the relative toughness data resulting from Charpy impact testing and other earlier testing methods. However, except for a few workers,[1-9] these new analytical techniques have rarely been used to their full potentials, for the following reasons:

1. Not many researchers have combined electron microscopy and fracture toughness testing in the study of a single alloy system in order to relate structure to mechanical properties. Often there exists either toughness data or structural information for an alloy, but not both.
2. A large share of structural steel research is devoted to the study of commercial alloys having complex compositions. The number of metallurgical variables in these steels and the possible interactions between multiple alloying elements make it extremely difficult to reach any conclusions about the effects of a single element on material properties. There is a need for more work on simple ternary alloys of iron, carbon, and one alloying element. With all other parameters held constant, the relations between a single alloying element and structural/mechanical properties can then be determined. It is most important in this respect to fix the carbon level, since it is known that variations in carbon will cause major changes in martensitic microstructure and mechanical properties.

An attempt has been made over the last several years to rectify this situation, and provide insight into the effects of single element additions on martensitic substructure and mechanical properties.[10] The present work on Fe/Cr/C steels is part of this continuing study, which so far has investigated the changes in material properties produced by additions of nickel, manganese, and cobalt.[4,8-10] Studies are also proceeding on Fe/Mo/C steels (Clarke--in progress).

One of the fundamental controversies in structural steel research concerns the effects of martensitic transformation twins on mechanical properties. Historically, the first thin film studies of martensite were performed by Kelly and Nutting in 1959/60.[11,12] They drew attention to the presence of transformation twins in high carbon steels, and in 1960 were the first to propose that twins could raise the yield strength.[12(a)] Since then, there have been numerous conflicting reports in the literature regarding the influence of transformation twins on mechanical properties. For example, while some authors state that twins can increase the flow strength of martensite,[3,10,11] others maintain that there is no connection between the amount of twinning and flow strength.[1.13] These issues are as yet unresolved mainly because of the complex substructure of martensite, which creates difficulties in analysis. The microstructural correlations were very incomplete during the period (1960-66) when many of these theories were developed. Furthermore, the myriad other variables, such as autotempering, retained austenite, impurities, and alloying elements in solid solution, must be controlled if one is to reach valid conclusions regarding the effects of transformation twins on mechanical properties. The significance of twinning in fracture toughness was emphasized by Tetelman[14]

in a discussion of the ausforming results obtained by Thomas et al.,[15] who showed that increases in strength and toughness could be achieved by ausforming. He stated that mechanical twinning in BCC metals favors crack nucleation, and that high (unpinned) dislocation densities inhibit twinning and crack nucleation. Hence, as a design parameter, twinning modes of deformation in martensite should be avoided. The effects of composition on substructure must be completely understood and controlled[10] if one is to produce martensitic steels with desirable mechanical properties.

As part of the continuing program involving a systematic study of the common alloying elements in steels and how they affect metallurgical properties,[4,8-10] the present work examines the structure and mechanical properties of Fe/Cr/C martensitic steels. This simple, ternary alloy system is of special interest because, even though chromium is a common alloying element, there has been little research on whether chromium additions can alter the martensitic substructure and toughness. Another reason for studying the Fe/Cr/C system is that chromium is known to be an ineffective solid solution strengthener in ferritic alloy steels.[16,17] Thus, correlations can more readily be established between any substructural changes (produced by chromium additions) and changes in mechanical properties, without having to consider any contributions to strength from chromium in solid solution. Finally, at carbon levels below 0.45 wt.%, Fe/Cr/C steels with up to 12 wt.% Cr can be fully austenitized. This allows the chromium content to be varied over a wide range, increasing the likelihood of obseving any structural change produced by chromium additions. This alleviates the sort of problem faced by Das and Thomas[9] in their work on Fe/Ni/Co/C steels. The gamma loop

for their alloys was not as wide as in chromium steels, and carbon content had to be changed in order to alter the martensitic substructure. Consequently, it was not clear whether the observed differences in toughness between alloys were due to changes in substructure or changes in carbon level, even in alloys with the same yield strength. The four to 12 wt.% Cr range was chosen to provide a reasonable chance of observing any structural change which chromium might induce, while having sufficient hardenability in all the alloys.

This study of Fe/Cr/C steels seeks answers to the following questions:

1. For a given carbon level, does an increase in chromium concentration produce transformation twinning in martensite?
2. If so, will such twinning have any effect on strength and toughness?
3. On tempering at various temperatures, how are changes in martensite substructure and carbide morphology related to changes in mechanical properties?

This research was also carried out with the aim of designing low cost strong, tough, steels by design and control of microstructure.

## II. EXPERIMENTAL PROCEDURE

### A. Material Preparation and Heat Treatment

The compositions and $M_s$ temperatures of the alloys used in this investigation are listed in Table I. $M_s$ temperatures were determined by dilatometric measurements. Note that the nominal composition is indicated by the alloy number: the first two and last two digits represent nominal wt.% Cr and wt.% C, respectively. The alloys were vacuum melted in 75 lb heats, forged, and hot rolled to 0.5 in. plate (for fracture toughness specimens) and 0.15 in. sheet (for tensile specimens). Alloy 0417 was rolled to 1.0 in. plate. It was felt that this extra thickness would be required to obtain plane strain fracture toughness conditions in this low alloy steel. All pieces were sandblasted to remove oxide scale, homogenized under vacuum at 1200°C for 48 hours, and furnace cooled. Tensile and fracture toughness specimen blanks cut from the plates were austenitized in an argon atmosphere at 1100°C for one hour, quenched in agitated oil, and transferred to liquid nitrogen to ensure complete transformation to martensite. Later X-ray diffractometer examination showed no evidence of retained austenite. The high austenitizing temperature of 1100°C was chosen so that all carbides would be dissolved prior to quenching. It was verified by electron metallography that the as-quenched specimens were free of undissolved carbides. The high temperature also produced very large austenite grains ($\simeq$ 230 μm diameter) in all the alloys.

While some specimens of each alloy were used to determine as-quenched mechanical properties, others were tempered at 200, 400, and 600°C in a neutral salt bath for one hour and oil quenched. The carbon concentrations whown in Table I were obtained from specimens which had gone through the

entire heat treatment sequence. Since alloy 0417 was thicker than the others and had the lowest alloy concentration, it was the one most likely to have insufficient hardenability in the fracture toughness specimens. Vickers microhardness readings were therefore taken through the cross-section of a 1.0 in. thick heat treated sample of alloy 0417 whose dimensions were similar to those of the fracture toughness specimens. These readings were constant through the thickness, indicating complete transformation to martensite, and confirming that no decarburization had occurred. Electron microscopy later showed no evidence of isothermal transformation products in any of the alloys.

### B. Electron Microscopy

After mechanical testing, 0.015 in. thick sections were cut from the undeformed part of fracture toughness specimens, and ground to 0.005 in. thickness. Foils for transmission electron microscopy were prepared from these pieces by the window method, using the standard chromic-acetic acid electrolyte (75 gm $CrO_3$, 400 cc acetic acid, 21 cc $H_2O$). The polishing voltage varied from 15 to 25 volts, depending on the alloy and tempering treatment. Electrolyte temperature was maintained between 12 and 15°C. Foils were examined in a Siemens Elmiskop IA at an accelerating voltage of 100 kV, utilizing quantitative methods of analysis, such as high resolution dark field imaging and stereo microscopy.

### C. Mechanical Testing

After heat treatment, final machining was performed on all mechanical test specimens. Approximately 0.02 in. was removed from all flat surfaces to get rid of any decarburized layer. Optical microscopy revealed that decarburization was never any deeper than 0.005 in. For the 0.17 wt.% C

alloys, flat tensile specimens (Fig. 1A) were used to obtain strength and percent elongation data. Due to a difference in carbon levels between the plate and sheet of alloy 0435, it was necessary to use round tensile specimens (Fig. 1B) taken from the same 0.5 in. plate as the fracture toughness specimens in order to have strength and toughness data for this alloy correspond to the same wt.% C. Alloy 1235 was found to be extremely brittle, such that the tensile specimens failed before yielding. It was therefore necessary to use compression specimens (Fig. 1C) to determine the yield strength of this alloy. Since the material was tested in compression, ultimate tensile strength and percent elongation were not obtained.

Plane strain fracture toughness testing was carried out using the compact tension crackline loaded specimen shown in Fig. 1D. Specimen thicknesses varied, depending on the estimated minimum thickness required to produce plane strain conditions in a given alloy. Specimens were fatigue precracked to form a sharp initial crack between 0.05 and 0.01 in. long.

Flat tensile specimens were tested at room temperature in a 5000 Kg capacity Instron testing machine, at 0.1 cm/min crosshead speed. All other mechanical testing was alone at room temperature in a 300 kip capacity MTS testing machine at a loading rate of 0.04 in./min. From the fracture toughness test results, critical stress intensity values were calculated in accordance with ASTM standards.

# III. RESULTS

## A. Structure of As-Quenched Martensite

Kelly and Nutting[11,12] first showed how the martensitic substructure depends on carbon content and ($M_s$-$M_f$) temperature in plain carbon steels. At low carbon levels (less than 0.15 wt.% C) the martensite consists of bundles of heavily dislocated laths. Adjacent laths are sometimes twin related or separated by small angle boundaries.[12,18] At high carbon levels (over 0.8 wt.% C) the substructure is mainly plates containing transformation twins. The majority of structural steels have carbon contents between these two extremes, and their substructures are mixtures of dislocated laths and twinned plates. A mixed morphology was found in all the Fe/Cr/C steels investigated in the present work. The morphologies varied from mainly dislocated laths with little twinning to equal amounts of laths and twinned plates, depending on the carbon and chromium concentrations. It was found that additions of either carbon or chromium increased the percentage of martensite containing transformation twins. The method used to determine the relative fractions of twinned martensite was similar to that used by Liu[5] in analysing HP9-4-45 martensite. A large number (at least 40) of random orientation bright field electron micrographs was taken for each alloy in the as-quenched condition. The fraction of twinned martensite grains in each micrograph of a given alloy was determined visually, and average fractions computed. Using the average fraction of twinned martensite in alloy

0417 as a base level(n), the values for the other alloys were referenced to this level as multiples of n in order to determine relative amounts of twinning among the various alloys. These relative values are shown in Table I. Although this is a crude measurement of the amount of twinning, it is the only method presently available. The estimates are undoubtedly less than the actual percentages of twinned martensite, since only a fraction of all the twins are in contrast in one foil orientation. It has been estimated that for a given foil orientation, only about one out of six of the twins actually present will be visible.[3,11,12]

1. 0.17 wt.% C - X wt.% Cr Martensites

As seen in Fig. 2A, the low carbon martensites contained mostly dislocated laths with few twins. However, even though the twin density was low in all three 0.17 wt.% C alloys, there was a noticeable rise in the relative fraction of twinned martensite from n to 5n as chromium content increased from 4 to 12 wt.%. Figure 2B,C shows an example of the transformation twins found in the low carbon alloys. Lath widths in all alloys varied from 0.1 to 2$\mu$.

The degree of autotempering (precipitation of $Fe_3C$ in martensite during quenching) also depended on chromium content. The density of autotempered carbides was highest in the 4 wt.% Cr alloy and decreased at higher chromium levels. An example of autotempered carbide morphology is shown in Fig. 3A, B. This is similar to the autotempering observed by Page,et.al.[19] in Fe-3.6Cr-0.19C martensite. The carbides form a Widmanstatten pattern parallel to $\{110\}_\alpha$ which indicates they

are $Fe_3C$, based on earlier reports in the literature[4,8,9,12,19] on the habit plane of $Fe_3C$. Figure 3B is a dark field image of the (110) variant of $Fe_3C$. There was also evidence of autotempered $Fe_3C$ in the matrix regions of some martensite plates which also contained twins (see Fig. 3C). This does not agree with earlier results of Kelly and Nutting[12] stating that the presence of autotempering in a martensite grain indicates that the martensite does not contain twins.

2. 0.35 wt.% C - X wt.% Cr Martensites

Alloys 0435 and 1235 showed the greatest difference in the relative amounts of twinned martensite. Although both alloys had a mixed structure of dislocated laths and twinned plates, there was a clear increase in observable twin density by a factor of approximately two between the 4 wt.% Cr alloy and the 12 wt.% Cr alloy. Note that both of these alloys have the same carbon concentration. These results, in conjunction with the analysis of martensitic substructure in the 0.17 wt.% C alloys, demonstrate conclusively that chromium induces transformation twinning in martensite. Figures 4(A,B) and 4(C,D) show the typical substructures found in alloys 0435 and 1235, respectively. In some cases the twins appear as long needles (Fig. 4B), while in others they are more truncated (Fig. 4C). Both types of twins were equally common to both alloys.

The other significant difference between the 0.35 wt.% C alloys is that only alloy 0435 exhibited autotempering (see Fig. 5). Although a careful search was conducted to detect autotempering in alloy 1235, none could be found. The extent of autotempering in alloy 0435 was

very low, and carbides were found only in scattered regions of the foil. The density of autotempered carbides in alloy 0435 was much less than that found in any of the 0.17 wt.% C steels.

## B. Structure of Tempered Martensite

The carbide morphologies produced on tempering were clearly linked to the martensitic substructure. In untwinned martensite, the carbides precipitated in Widmanstatten patterns within the martensite laths or as sheets at lath boundaries, depending on the tempering temperature. If transformation twins were present, carbides formed along twin/matrix interfaces. At high temperatures (600°C), $Fe_3C$ tended to coarsen and spheroidize, and in some of the alloys, $Cr_7C_3$ formed as a fine platelet dispersion within martensite grains.

### 1. Tempering at 200°C

In the 0.17 wt.% C alloys there was little difference in carbide morphology or density between the as-quenched specimens and those tempered at 200°C. The one difference was that at 200°C, $Fe_3C$ precipitated along twin boundaries, whereas in the as-quenched condition no twin boundary carbides were present. This was not a major distinction, however, since the existing twin density in these alloys was low. As in the as-quenched specimens, the principal carbide morphology was a Widmanstatten pattern of $Fe_3C$, as seen in Fig. 6B,C.

The 0.35 wt.% C alloys showed a different response to 200°C tempering, depending on the chromium content. Alloy 0435 exhibited a much greater number and a slight coarsening of the Widmanstatten

carbides (Fig. 6A), and formation of $Fe_3C$ along twin boundaries. Alloy 1235 displayed the greatest change in carbide distribution and density on tempering, from no carbides in the as-quenched condition to a very fine dispersion of epsilon carbide on $\{100\}_\alpha$ planes after 200°C tempering (see Fig. 7A). Based on earlier reports in the literature,[4,8,9,12] it is reasonable to conclude that carbides parallel to $\{100\}_\alpha$ in martensite are epsilon carbide. It is almost impossible to distinguish between $Fe_3C$ and epsilon carbide by electron diffraction patterns, since the d-spacings of these carbides are very similar. Very few twin boundary precipitates were observed in alloy 1235 after 200°C tempering.

2. Tempering at 400°C

The 0.16 wt.% C alloys continued to show little coarsening of Widmanstatten carbides; as shown in Fig. 8C. However, carbide sheets began forming along interlath boundaries at 400°C (see Fig. 8A,B). These interlath precipitates were not very prevalent in the low carbon alloys. There was virtually no growth or coarsening of the twin boundary carbides.

Alloys 0435 and 1235 also contained lath boundary carbides (Fig. 9A, B), in addition to the twin boundary precipitates seen at 200°C. Figure 7B-D is a typical example of the twin boundary carbide morphology found in all the alloys after 200 or 400°C tempering. At 400°C, the Widmanstatten $Fe_3C$ in alloy 0435 experienced further coarsening (Fig. 9C), whereas in alloy 1235 the epsilon carbide was replaced by $Fe_3C$ on $\{110\}_\alpha$ planes (Fig. 9D). Furthermore, the twin

boundary precipitates in alloy 1235 were more prevalent at 400°C than at 200°C.

3. Tempering at 600°C

All the precipitates observed at lower temperatures were coarsened and spheroidized at 600°C. Figure 10 shows segmented lath and twin boundary carbides in alloy 0435. Segmentation of lath boundary carbides also occurred in the low carbon alloys, as seen in Fig. 11D. Existing precipitates within the martensite laths were spheroidized at 600°C, and some recovery and recrystallization was evident in all the alloys (see Fig. 11). On the other hand, a new, finely dispersed precipitate had formed within the martensite laths, as shown in Fig. 12. Earlier work by Honeycomb et.al.[20] and Page et.al.[19] concludes that this high temperature precipitate is $Cr_7C_3$. These fine carbide dispersions were observed only in isolated regions of the foil.

## C. Presence of Retained Austenite

One of the most interesting aspects of the electron microscopy studies was the discovery of thin sheets of highly deformed retained austenite surrounding some of the martensite laths in all the as-quenched alloys. These interlath sheets were identified as austenite by dark field imaging and analysis of selected area diffraction patterns. Figure 13 shows an example of martensite laths surrounded by retained austenite in alloy 0817. Figure 13B is the dark field image of an FCC diffraction spot, illuminating the retained austenite boundaries. On tempering at 200°C, the interlath austenite was

observed less frequently, and after tempering at 400°C none was seen, indicating that tempering causes the retained austenite to transform to ferrite, followed by precipitation of interlath carbides.

## D. Mechanical Properties

The mechanical properties vs. tempering treatment of all the alloys are summarized in Table II and plotted in Figs. 14 through 16. In the 0.17 wt.% carbon alloys, there was essentially no difference in as-quenched yield strength among the three chromium levels, confirming that chromium is not a solid solution strengthener in steel. However, in the 0.35 wt.% C alloys, yield strength increased sharply from 240 to 300 KSI between the 4 and 12 wt.% Cr alloys. To eliminate the possibility that the strength differential was related to the difference in testing method (tension for alloy 0435 vs. compression for alloy 1235), alloy 0435 was also tested in compression. This produced the same yield strength as in tension, of 240 KSI. Since the yield strength data for the low carbon alloys eliminate chromium as a solid solution strengthener, some other explanation must be sought for this marked increase in strength with chromium addition. This will be discussed in the next section.

The 0.17 wt.% carbon alloys demonstrated a pronounced resistance to softening on tempering. There was little decrease in hardness or strength up to a tempering temperature of 400°C (see Figs. 14 and 15). Above this temperature hardness and strength dropped sharply. A more normal response to tempering was found in the 0.35 wt.% C alloys, as

seen in Figs. 14 and 16. Hardness and strength decreased linearly with tempering temperature up to 400°C, and exhibited significant softening after tempering at 600°C. The yield strength differential between alloys 0435 and 1235 decreased steadily with increasing tempering temperature, until there was little difference in strength at 600°C.

The as-quenched fracture toughness of the 0.17 wt.% C alloys decreased somewhat with chromium additions, from 83 KSI-in.$^{1/2}$ (alloy 0417) to 68 KSI-in.$^{1/2}$ (alloy 1217). There was no difference in as-quenched toughness between alloys 0417 and 0817, although alloy 0817 failed to meet all the plane strain fracture toughness criteria so that the actual $K_{1c}$ for this alloy may be slightly lower than 83 KSI-in.$^{1/2}$. The dependence of as-quenched fracture toughness on chromium content was much more dramatic in the 0.35 wt.% C alloys, as seen in Fig. 16. When the chromium level increased from 4 to 12 wt.%, the as-quenched fracture toughness dropped from 70 to 20 KSI-in.$^{1/2}$. The brittleness of alloy 1235 was also indicated by the presence of quench cracks along prior austenite grain boundaries. These were not encountered in alloy 0435. The majority of the quench cracks were removed by surface grinding the $K_{1c}$ specimens of alloy 1235 before testing; this is the reason for the reduced thickness of these specimens indicated in Fig. 1. Scanning electron fractography was used to verify that the quench cracks did not influence the measured fracture toughness of alloy 1235. The fracture path was transgranular, and not along prior austenite grain boundaries.

The toughness of all the alloys increased after tempering at 200°C. The gain in toughness was more pronounced in the alloys with higher chromium contents. For example, 200°C tempering caused toughness to increase from 83 to 92 KSI-in.$^{1/2}$ in alloy 0417, versus a larger gain from 68 to 117 KSI-in.$^{1/2}$ in alloy 1217. On tempering at 400°C, toughness declined from the 200°C tempering levels in all alloys except 1235, which experienced no change in toughness between these two tempering treatments. 600°C tempering produced substantial gains in toughness in all the alloys. Except for alloy 1235, this does not seem to be indicated by the $K_{1c}$ data plotted in Figs. 16 and 17. The discrepancy was due to the $K_{1c}$ specimens being not nearly thick enough to meet plane strain conditions at the high toughness levels. Plastic flow at the root of the fatigue crack and slow crack growth occurred at relatively low loads, and the fracture surfaces consisted mainly of shear lips. This behavior on testing in conjunction with the graphical method of computing stress intensity factors resulted in the erroneous fracture toughness values. The actual ductility is better represented by the percent elongation curves, which rise steeply on tempering at 600°C.

The validity of $K_{1c}$ results was determined by using the ASTM standard procedures for checking the linearity of the load/crack opening displacement curves up to the point of crack propagation, and the requirement that specimen thickness must be greater than $2.5\left(\frac{K_{1c}}{\sigma_y}\right)^2$ for a valid $K_{1c}$ result. It was not possible to directly confirm the

$K_{1c}$ data by testing specimens of greater thickness (If plane strain conditions are being met the resultant stress intensity factor K should not change as thickness is increased). However, for the specimens which satisfied the ASTM requirements, plane strain conditions were also indicated by the flat fracture surfaces, the absence of shear lips or necking, and no evidence of a plastic zone at the root of the fatigue crack.

# IV. DISCUSSION

## A. Morphology of Martensite

There are various conflicting theories in the literature regarding the factors that determine whether the substructure of martensite consists of dislocated laths, twinned plates, or a mixture of both. While some authors contend that martensite substructure is controlled by the $M_s$ temperature (lowering of $M_s$ induces twinning),[3,11-13] others have argued that composition plays an important role, in that alloys of different compositions with similar $M_s$ temperatures can have completely different substructures.[8-10,21] A plausible interpretation of the controversy, which consider the importance of both $M_s$ temperature and composition, have been proposed by Thomas[10] and by Krauss and Marder.[18] They submit that composition determines substructure through its effects on $M_s$ temperature and strength of martensite. Since most alloying elements act as solid solution strengtheners in austenite, they increase the thermodynamic driving force necessary to initiate the martensitic shear transformation, and hence lower the $M_s$ temperature. The strength of the martensite at the temperature of transformation then becomes the controlling factor: whether the martensite slips or twins depends on the critical resolved shear stress (CRSS) for slip versus twinning at the temperature of transformation.[10] If the CRSS for slip is less than that for twinning, the martensite will slip, and vice versa. Since martensite forms through a temperature range of approximately 200°C during the quench, and the

CRSS for slip in BCC martensite increases as temperature decreases, the relative magnitudes of the CRSS for slip and twinning may be reversed at the beginning and end of the martensitic transformation. An alloy may therefore have a mixed substructure of dislocated and twinned martensite. At temperatures just below $M_s$, the CRSS for slip is less than that for twinning, and dislocated martensite forms. At lower temperatures, the CRSS for slip has increased to a stress higher than that for twinning, and the martensite formed near the end of the transformation is twinned. This is a reasonable explanation for the mixed substructures found in the present investigation. Alloy 0417 has the lowest chromium and carbon content, the highest $M_s$ temperature, and is mainly dislocated. Conversely, alloy 1235 with the greatest amount of chromium and carbon has the lowest $M_s$ temperature and the highest twin density. Chromium therefore has the same effect on martensitic substructure as carbon,[11] manganese[4] and nickel;[2] all these elements induce twinning.

The degree of autotempering is also determined by the alloying element concentration and the related $M_s$ temperature. In Fe/Cr/C alloys, there are three factors which can influence the extent of autotempering:

1. $M_s$ Temperature. At lower temperatures the diffusivity of carbon in martensite is significantly reduced, and the lower mobility of carbon will impede the precipitation of $Fe_3C$ during the quench. Since $Fe_3C$ cannot precipitate until after the martensite has formed, an alloy with a lower $M_s$ temperature should experience less autotempering.

2. Carbon Concentration. If additional carbon is added to an alloy, the martensite becomes more supersaturated with carbon, and autotempering should increase.

3. Chromium Concentration. As shown by Honeycombe,[17] an increase in chromium content retards the diffusivity of carbon, and should therefore reduce the amount of autotempering.

These three considerations are of course interrelated, in that $M_s$ temperature is affected by chromium and carbon content. However, in the alloys studied, $M_s$ temperature appeared to be the controlling factor. For instance, alloy 0417 had the highest $M_s$ temperature and the greatest amount of autotempering. In comparison, alloy 0435 had the same chromium content, additional carbon, and a lower $M_s$ temperature. The higher supersaturation of carbon which would promote autotempering was overshadowed by the retarded carbon diffusivity caused by the lower $M_s$. Consequently, autotempering was much less prevalent in alloy 0435 compared to 0417. The alloy with the lowest $M_s$ temperature exhibits no autotempering whatsoever.

1. Retained Austenite

The observations of retained austenite between martensite laths confirms some early work of Honeycombe et.al.,[20] in which he suggests that the absence of interlath carbides in Fe/Cr/C steels at tempering temperatures below 400°C is related to the possibility of austenite films at lath boundaries. He proposes that carbides do not form at the boundaries at low temperatures because of the higher solubility of carbon in austenite. On tempering at 400°C or higher, the austenite

films transform to more stable ferrite. Since the ferrite retains the carbon concentration of the austenite, which is higher than in the adjacent laths, $Cr_7C_3$ precipitates preferentially at 400°C along the interlath boundaries. This is precisely what was observed in the present study. The austenite films disappeared after tempering at 400°C, and were replaced by interlath carbides.

It was surprising to find retained austenite in alloys with such high $M_s$ temperatures, since the austenite to martensite transformation is normally completed at approximately 200 to 250°C below $M_s$. Kelly and Nutting[11] showed that austenite can be stabilized by partial transformation to martensite. The volume and shape changes accompanying the martensite transformation produce deformation in the surrounding austenite. They found dislocation densities as high as $10^{12}/cm^2$ in the austenite adjacent to martensite plates. This distorted lattice makes the cooperative movement of atoms necessary for further martensitic transformation more difficult, and the austenite is thereby stabilized. Furthermore, if dissolved carbon is highly concentrated locally in the interlath austenite films, then the $M_s$-$M_f$ temperature range is much lower in these regions than in the rest of the material. With a large amount of dissolved carbon in the lath boundaries, the $M_f$ temperature for these regions may be below room temperature, causing stabilization of the retained austenite films.

In applying this concept to the present work, it is not unreasonable that austenite could be retained as interlath films, even at temperatures well below the martensite finish temperature. The

austenite has been trapped between two martensite laths which have grown together, and is extremely heavily dislocated. A very high energy is then needed to transform the stabilized austenite to ferrite. This energy is not available until the alloy is heated to 400°C or above; at this temperature the austenite film is able to transform to ferrite. The lath boundary ferrite is then highly supersaturated with carbon (since it retains the carbon concentration of the austenite) and the observed interlath carbides form.

### B. Carbide Distribution in Tempered Martensite

The response of the alloys to tempering was almost completely determined by the martensitic substructure and the degree of prior autotempering. Kelly and Nutting[11] first pointed out this dependence of carbide morphology on martensitic substructure in plain carbon steels. The tempering results of the present study are very similar to those of other investigators,[7,9,22-25] especially the work of Seal and Honeycombe.[20] The 0.17 wt.% C alloys had undergone so much autotempering, due to their high $M_s$ temperatures, that there was little change in matrix carbide distribution or density after tempering up to 400°C. The only differences in carbide morphology in these alloys were the formation of twin boundary carbides at 200°C and interlath carbides at 400°C. The most significant feature of the tempering behavior of these alloys was the absence of matrix carbide coarsening at temperatures up to 400°C. This is most likely due to chromium retarding the diffusivity of carbon.[17]

The 0.35 wt.% C alloys responded differently to tempering, in that there was a large increase in the number of carbides at 200°C compared to the number present in the as-quenched state. Since there was minimal or nonexistent autotempering, the alloys were still highly supersaturated with carbon, so that even tempering as low as 200°C produced an appreciable rise in the number of carbides. Alloy 0435 had little resistance to coarsening because of its low chromium and high carbon levels. Alloy 1235 was unusual in that it was the only one to form epsilon carbide at 200°C. This agrees with the results of Das and Thomas,[9] which conclude that, at 200°C or below, epsilon carbide precipitates in the dislocated regions of heavily twinned martensites, and $Fe_3C$ precipitates in a Widmanstatten pattern in dislocated martensites or on {112} twin interfaces. The replacement of epsilon carbide by $Fe_3C$ on $\{110\}_\alpha$ planes after tempering above 200°C has also been previously reported.[9,24]

The precipitation of $Fe_3C$ on twin boundaries is a common occurrence in tempered martensites.[2,4,8,20,22-24] Twin boundary carbide formation did not depend on composition. Whatever twins were present acted as favorable sites for carbide nucleation. Similarly, lath boundary carbides formed in all the alloys at 400°C or higher, regardless of composition or martensitic substructure. This suggests that twin and lath boundaries are the most expedient sites for heterogeneous nucleation and will dominate other locations provided the martensite is held long enough at a temperature high enough for chromium and carbon to diffuse to the boundaries. The lack of time at temperature is the reason why

boundary carbides are not formed during quenching. Autotempering must occur so rapidly that the carbon can move only short distances, and the autotempered carbides precipitate on dislocations within the laths in a Widmanstatten pattern. As was previously discussed, autotempering at lath boundaries will also be prevented by the presence of retained austenite films.

All the alloys were reduced to essentially the same structure after 600°C tempering. Twin and lath boundary carbides became segmented, and matrix carbides were spheroidized. Seal and Honeycombe[20] report that $Cr_7C_3$ begins to replace $Fe_3C$ as low as 400°C, and by 600°C, it is the dominant precipitate. The rapid coarsening and loss of coherency between the carbides and the matrix is due to the high diffusivity of chromium at this temperature.[17,26,27] This seems to contradict the observations of scattered regions of fine carbide dispersions after 600°C tempering. However, the predominant carbide morphology was spheroidized lath boundary precipitates, and it has been shown[20] that these rapidly grow at the expense of the fine carbide dispersions within the laths. The occurrence of dislocation network recovery and the onset of recystallization also promoted the normalization of structure in all the alloys. In essence, after tempering at 600°C, there was no distinction in alloy substructure related to whether the as-quenched martensites were dislocated or twinned.

## C. Relations Between Martensitic Structure and Mechanical Properties

The heart of this investigation lies in understanding how the strength and toughness of Fe/Cr/C martensitic steels are affected by substructure when other variables which could influence mechanical properties, such as carbon level, are held constant. Cohen[13] has pointed out that in general, the high strength associated with martensite is due to interstitial solid solution strengthening by carbon, and the complex martensitic substructure. Several workers[1,2,13] have observed that in Fe/Ni/C alloys, a change in martensitic substructure from dislocated laths to twinned plates produced by increasing the nickel content causes no change in yield strength. Others[3,11,12] report a pronounced dependence of yield strength on twin density in steels with lower alloy contents. Kelly and Nutting[11,12] contend that transformation twins increase the hardness and strength of martensite. They show that the presence of twins reduces the number of available slip systems by a factor of four, since operative slip systems must be common to the twins and the matrix. The only deformation systems which meet this condition are the transformation twinning direction and the slip or twin planes lying in the zone of this direction. Furthermore, the sigmoidal shape of the as-quenched hardness versus carbon content curve[12] can be explained if the influence of twins on hardness is taken into consideration. If the hardness of martensite depended only on carbon content, the curve would be linear. The increase in twin density with carbon level between 0.15 and 0.8 wt.% C can account

for the actual shape of the curve. At high carbon levels, retained austenite reduces the hardening effects of carbon and twins, and the curve begins to flatten out. Das and Thomas[28] showed, using high voltage electron microscopy, that double twinning can occur (where the twins themselves are twinned). This can further add to the hardening effect of twins. It has also been demonstrated that twinning induced by shock loading increases the hardness of FCC single component systems, such as nickel.[29]

These views are substantiated by the results of this research. In Fig. 17, yield strength, fracture toughness, and relative fraction of twinned martensite are plotted as functions of chromium concentration for both the 0.17 and 0.35 wt.% C alloys in the as-quenched condition. The relative fraction of twinned martensite in the 0.17 wt.% C alloys increases from n to 5n over the 4 to 12 wt.% range of chromium concentration. This is not a substantial increase in twin density, since all three alloys are only lightly twinned. For all three alloys, the substructure is mainly dislocated laths, so that plastic flow would not be significantly impeded by twins. As a result, since chromium is not an effective solid solution strengthener,[16,17] yield strength is essentially constant and independent of chromium content. Fracture toughness is mildly related to chromium level, and hence, twin density. In comparing the 8 and 12 wt.% chromium alloys, when the amount of twinned martensite increases from 2.5n to 5n, as-quenched toughness falls from 83 to 68 KSI-in$^{1/2}$. Thus, in two alloys with the same carbon content and yield strength, an increase in transformation twin

density lowers the plane strain fracture toughness.

The dependence of hardness, strength, and toughness on the amount of twinning for a given carbon concentration is much more obvious in the 0.35 wt.% C alloys. Raising the chromium level from 4 to 12 wt.% increases the relative fraction of twinned martensite by a factor of almost two. This causes Rc hardness to increase from approximately 50 to 62 (see Fig. 14). The most dramatic effects are seen in the strength and toughness curves of the 0.35 wt.% C alloys in Fig. 17. The increase in twinning between alloys 0435 and 1235 results in a rise in yield strength from 240 to 300 KSI. and a sharp drop in fracture toughness from 70 to 20 KSI-in.$^{1/2}$. Although the yield strengths are different, transformation twins are therefore seen to seriously impair the fracture toughness of Fe/Cr/C martensite at a constant carbon level. This is similar to the effect of twins on toughness in Fe/Ni/Mn/C martensite reported by Huang and Thomas.[4] Figure 18 shows that in conjunction with the difference in toughness, alloys 0435 and 1235 exhibited dissimilar fracture modes. The fracture surface of alloy 0435 consisted mainly of dimpled rupture, whereas there was a significant amount of cleavage in alloy 1235. This is the normal association of dimpled rupture with high toughness and cleavage with low toughness.

It is also evident in Fig. 17 that an increase in yield strength does not necessarily lead to lower toughness in martensite. The as-quenched yield strength of alloy 0435 is 84 KSI higher than that of alloy 1217, yet both have the same fracture toughness. The increased carbon content of alloy 0435 raises its yield strength over that of

alloy 1217, while the simultaneous reduction in chromium prevents a large increase in twinning and a drop in toughness. Hence, by manipulating the concentrations of carbon and alloying elements, the strength of martensitic steels can be improved without suffering a loss of toughness.

It could be argued that the strength and toughness differentials in alloys 0435 and 1235 resulted from variations in amounts of autotempering. However, this does not seem reasonable, since the difference in degree of autotempering was actually very slight and could not account for the major changes in mechanical properties. While alloy 1235 experienced no autotempering, the density of autotempered carbides in alloy 0435 was very low, and they were present in only scattered regions. It may be that carbon segregates to twin boundaries during quenching. The buildup of carbon would impede dislocation motion across twin boundaries. In an alloy with a high twin density (such as 1235) this would increase the yield strength, retard plastic flow at crack tips, and thereby lower the toughness. This proposed mechanism cannot be verified in the present investigation, since segregation of carbon without the formation of actual precipitates is not visible in the electron microscope. However, the subsequent formation of twin boundary carbides on tempering at 200°C is a good clue that carbon was originally segregated at the twin boundaries.

In considering the experimental results for the tempered specimens, there is once again a direct correlation between structure and mechanical properties, as illustrated in Figs. 14 through 16. The 0.17 wt.% C

alloys with dislocated substructures exhibit little change in carbide density on tempering up to 400°C, and consequently, softening and reduction in strength are retarded in this temperature range. The 0.35 wt.% C alloys, which had little or no autotempering, show a linear decrease in hardness and strength on tempering up to 400°C, which is associated with increased precipitation of carbides. Tempering at 600°C creates similar structures in all the alloys, and roughly similar reductions in hardness and strength and increases in toughness.

All alloys showed a reduction or leveling off of toughness at 400°C, associated with the formation of interlath carbides. This is analagous to the results of several other authors[4-7] concerning the embrittling effect of lath boundary carbides in martensite. The interlath austenite films may be beneficial in that they prevent formation of these lath boundary carbides at temperatures below 400°C.

Figure 19 compares the yield strength and fracture toughness of mainly dislocated with mainly twinned martensites. Points are plotted for each alloy under all heat treating conditions. Alloy 1235 is classified as twinned martensite. and all others as dislocated. It is evident that at the same yield strength, twinned martensites are always surpassed in toughness by dislocated martensites. This is especially obvious in comparing alloys 1235 and 0435 which have the same carbon content. This presentation further illustrates the detrimental effect of transformation twins on fracture toughness.

## D. Development of an Economical, Tough, Ultra High Strength Steel

An important result of this research is further experimental evidence that as-quenched martensites are not necessarily brittle. It has long been assumed by many metallurgists that martensite must always be tempered after quenching to raise toughness to a usable level, and that the consequent reduction of strength on tempering is therefore unavoidable. However, in the present case none of the 0.17 wt.% C alloys are brittle in the as-quenched condition. Furthermore, alloy 0485, with a plane strain fracture toughness of 70 KSI-in$^{1/2}$ and yield strength of 240 KSI, qualifies as an ultra high strength, high toughness steel in the as-quenched condition. Its toughness is improved without a serious loss in strength when tempered at 200°C. Goolsby et.al.[30] found similar high strength and toughness in as-quenched, autotempered, Fe-0.3C-5Mo martensite. Figure 20 compares the ultimate tensile strength and fracture toughness of this alloy with several commercial ultra high strength steels.[31] It shows that alloy 0435 matches or exceeds the properties of 18Ni maraging steel, the highest performance alloy presently available. It is also worth noting that alloy 0435 could undoubtedly be produced at a much lower cost than 18Ni maraging steel (or other steels, including molybdenum bearing alloys), considering the high cost of nickel versus the low cost of chromium and the relative amounts of alloying elements in the two steels.

## V. CONCLUSIONS

Based on this study of the structure and mechanical properties of Fe/Cr/C martensitic steels, the following conclusions are offered:

1. An increase in chromium or carbon content lowers the $M_s$ temperature and induces transformation twinning in martensite.
2. Chromium is not a solid solution strengthener in ferrous martensites. It strengthens by modifying the transformation substructures.
3. At a given carbon level, a higher percentage of twinned martensite causes an increase in hardness and strength and a reduction in plane strain fracture toughness. Dislocated martensites are therefore generally tougher than twinned martensites at comparable yield strengths.
4. The degree of autotempering is determined mainly by $(M_s-M_f)$ temperature; alloys with the lowest $M_s$ temperatures have the least amount of autotempering.
5. The carbide morphology produced on tempering up to 400°C is related to the extent of prior autotempering and martensite substructure. Highly autotempered alloys show little change in carbide density after tempering at or below 400°C, and consequently little reduction in hardness and strength.
6. In twinned martensite, at temperatures up to 400°C, carbides precipitate along transformation twin boundaries.

7. Tempering at 400°C produces carbides along martensite lath boundaries which lower the fracture toughness. This appears to be related to the presence of retained austenite films at the lath boundaries, which transform to ferrite at this temperature.
8. Tempering at 600°C leads to coarsening and spheroidization of carbides, recovery of dislocation substructures, and the beginning of recrystallization. This results in significant decreases in hardness and strength, and increases in toughness.
9. The toughness of as-quenched martensites appears to depend on the transformation substructure (which probably affects the mode plastic deformation). Tough Fe/Cr/C martensites can be obtained by minimizing twinning.

ACKNOWLEDGEMENTS

The author is indebted to Professor Gareth Thomas for his extensive guidance and encouragement throughout the course of this work. Special thanks are due Ms. Margaret Robson for her patient instruction and assistance in the electron microscopy studies. Dr. Frank Hultgren and Republic Steel Research Center graciously supplied the alloys used in this research, as well as extensive technical assistance. Appreciation is also extended to Professor Charles J. McMahon, Jr. at the University of Pennsylvania for many helpful discussions.

This work was performed under the auspices of the United States Atomic Energy Commission, through the Inorganic Materials Research Division of the Lawrence Berkeley Laboratory.

## REFERENCES


1. C. L. Magee and R. G. Davies, Acta Met., 19, 345 (1971).
2. M. Raghavan, University of California, (Ph.D. thesis), LBL-477, March 1972.
3. P. M. Kelly, in Electron Microscopy and Strength of Crystals, eds. G. Thomas and J. Washburn (John Wiley and Sons, New York, 1963) p. 917.
4. D. Huang and G. Thomas, Met. Trans., 2, 1587 (1971).
5. Y. H. Liu, Trans. ASM, 62, 55 (1969).
6. R. D. Goolsby, University of Calffornia, (Ph.D. thesis), LBL-405, Nov. 1971. Also R. Goolsby, W. Wood, E. Parker, and V. Zackay, Electron Microscopy and Structure of Materials Eds. G. Thomas et.al. U.C. press 1972, p. 798.
7. A. J. Baker, F. J. Lauta, and R. P. Wei, Structure and Properties of Ultrahigh-Strength Steels, ASTM STP 370. (American Society for Testing and Materials, Philadelphia, 1965) p.3.
8. M. Raghavan and G. Thomas, Met. Trans., 2, 3433 (1971).
9. S. Das and G. Thomas, Trans. ASM, 62, 659 (1969).
10. G. Thomas, Met. Trans., 2, 2373 (1971).
11. P. M. Kelly and J. Nutting, JISI, 197, 199 (1961).
12. (a) P. M. Kelly and J. Nutting, Proc. Roy. Soc. London, A259, 45 (1960). See also (b) Kelly and Nutting, Physical Properties of Martenite and Bainite, ISI Spec. Rpt. No. 93, (The Iron and Steel Institute, London, 1965) p.166.

13. M. Cohen, Proceedings of the International Conference on the Strength of Metals and Alloys, Tokyo, Supplement to Trans. Japan Inst. of Metals, 9, XXIII (1968).

14. A. S. Tetelman, in High Strength Materials, ed. V. Zackay (John Wiley and Sons, New York, 1965) p. 325.

15. G. Thomas, D. Schmatz, and W. Gerberich, ibid. p. 251.

16. R. Honeycombe, Trans. Iron and Steel Inst. Japan, 6, (#5), 217 (1966).

17. R. Honeycombe, Metallurgical Developments in High-Alloy Steels, ISI Spec. Rpt. No. 86, (The Iron and Steel Institute, London, 1964) p.1.

18. G. Krauss and A. Marder, Met. Trans., 2, 2343 (1971).

19. E. Page, P. Manganon, G. Thomas, and V. Zackay, Trans. ASM, 62, 45 (1969).

20. A. Seal and R. Honeycombe, JISI, 188, 9 (1958).

21. O. Johari and G. Thomas, Acta Met., 13, 1211 (1965).

22. M. Wells, Acta Met. 12. 389 (1964).

23. G. Pellisier, Eng. Fracture Mech., 1, 55 (1968).

24. E. Tekin and P. M. Kelly, Precipitation from Iron-Base Alloys, eds. G. Speich and J. Clark (Gordon and Breach, New York, 1965) p. 173.

25. A. Baker, P. M. Kelley, and J. Nutting, in Electron Microscopy and Strength of Crystals, eds. G. Thomas and J. Washburn (John Wiley and Sons, New York, 1963) p. 899.

26. R. Honeycombe, H. Harding, and J. Irani, in High-Strength Materials, ed. V. Zackay (John Wiley and Sons, New York, 1965) p. 213.

27. F. Pickering, Precipitation Processes in Steels, ISI Spec. Rpt. No. 64, (The Iron and Steel Institute, London, 1959) p. 23.

28. S. Das and G. Thomas, JISI, 209, 801 (1971).

29. R. Nolder and G. Thomas, Acta Met., 12, 227 (1964).

30. V. Zackay, E. Parker, R. Goolsby, and W. Wood, Nature, 236, 108 (1972).

31. R. Ault, G. Waid and R. Bertolo, Tech. Rep. AFML-TR-71-27.

Table I. Chemical Compositions of Alloys

| Alloy Number | Composition, wt.% C | Cr | Si | O | $M_s$ Temp., °C | Relative fractions of twinned martensite |
|---|---|---|---|---|---|---|
| 0417 | 0.18 | 4.2 | 0.14 | 0.001 | 408 | n |
| 0817 | 0.16 | 8.4 | 0.15 | <0.002 | 358 | 2.5n |
| 1217 | 0.17 | 12.0 | 0.15 | <0.002 | 286 | 5n |
| 0435 | 0.35 | 4.0 | 0.06 | 0.003 | 320 | 9n |
| 1235 | 0.34 | 12.2 | 0.10 | 0.002 | 182 | 17n |

Table II. Mechanical Properties of Alloys

| Alloy Number | Tempering Temp., °C | $R_c$ Hardness | 0.2% offset Yield Strength, KSI | Ultimate Tensile Strength, KSI | Percent Elongation | Plane Strain Fracture Toughness $K_{1c}$, KSI-in.$^{1/2}$ |
|---|---|---|---|---|---|---|
| 0417 | as Quenched | 41.7 | 160 | 194 | 10.0 | 83 |
| | 200 | 41.6 | 166 | 195 | 9.5 | 92 |
| | 400 | 40.3 | 162 | 185 | 9.7 | 83 |
| | 600 | 21.2 | 91 | 106 | 15.0 | 77* ¤ |
| 0817 | as Quenched | 40.6 | 157 | 196 | 11.0 | 83* # |
| | 200 | 41.2 | 157 | 192 | 10.5 | 115* |
| | 400 | 40.3 | 154 | 182 | 10.5 | 88* |
| | 600 | 22.9 | 99 | 116 | 15.0 | 60* ¤ |
| 1217 | as Quenched | 45.0 | 156 | 214 | 9.0 | 68 |
| | 200 | 44.5 | 178 | 214 | 12.0 | 117* |
| | 400 | 42.2 | 162 | 200 | 11.5 | 82 |
| | 600 | 23.5 | 106 | 123 | 13.0 | 40* ¤ |
| 0435 | as Quenched | 49.9 | 240 | 306 | 5.0 | 70 |
| | 200 | 45.6 | 218 | 275 | 7.5 | 92* # |
| | 400 | 42.2 | 201 | 237 | 9.0 | 77 |
| | 600 | 25.5 | 126 | 149 | 17.0 | 45* ¤ |
| 1235 | as Quenched | 60.6 | 300 | | | 20 |
| | 200 | 56.3 | 252 | | | 41 |
| | 400 | 52.2 | 226 | | | 42 |
| | 600 | 32.3 | 118 | | | 73* |

*These are apparent toughness values (KQ) since they do not meet all the conditions specified in ASTM Standards for plane strain.

#These KQ values are very close to meeting plane strain conditions and hence are close approximations of $K_{1c}$.

¤These are anomalously low toughness values due to the lack of sufficient specimen thickness and the graphical methods of computing $K_{1c}$. The alloys tempered at 600°C were actually very ductile. Notice the percent elongation figures as an indication of high toughness at 600°C.

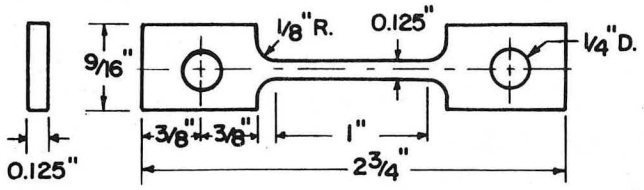


a. FLAT TENSILE SPECIMEN

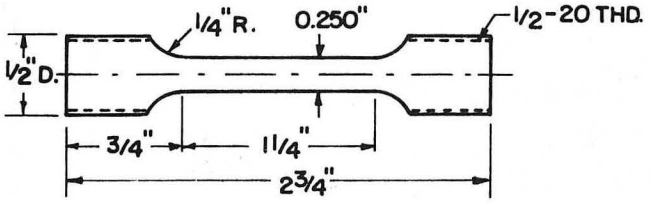


b. ROUND TENSILE SPECIMEN

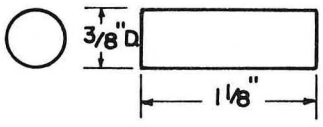


c. COMPRESSION SPECIMEN

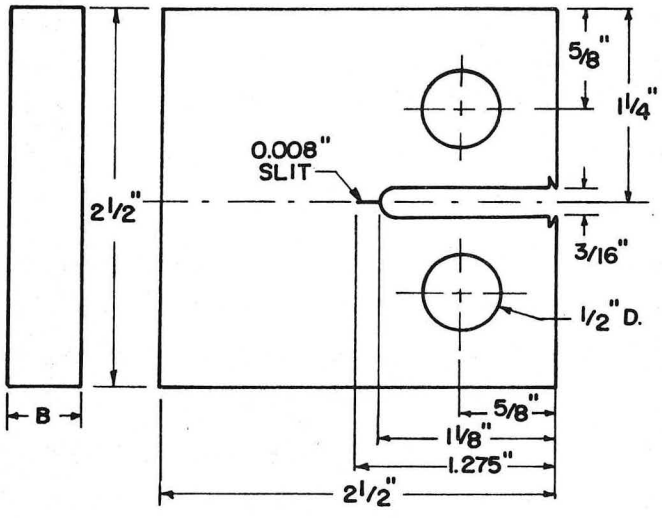


| ALLOY NO. | THICKNESS B, in. |
|---|---|
| 0417 | 0.920 |
| 0817 | 0.525 |
| 1217 | 0.525 |
| 0435 | 0.510 |
| 1235 | 0.350 |

d. FRACTURE TOUGHNESS SPECIMEN

XBL 7211-7160

Fig. 1. Mechanical test specimens used in this research.

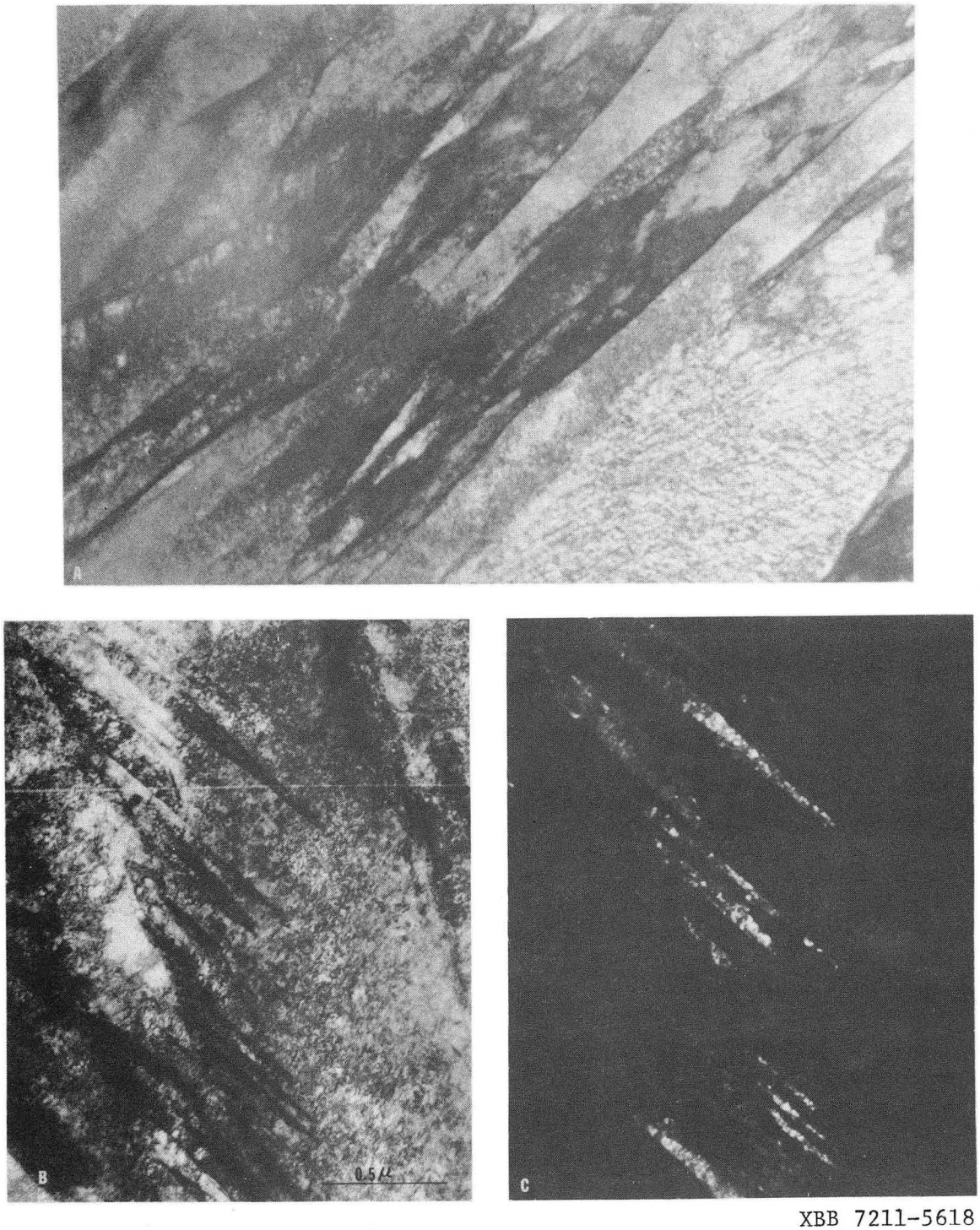


XBB 7211-5618

Fig. 2. As quenched structure of alloy 1217, showing wide variation in lath widths (a). (b) and (c) show the bright field and dark field of transformation twins in as-quenched alloy 0817. These micrographs are representative of the as-quenched structures of all the 0.17 wt.% C alloys.

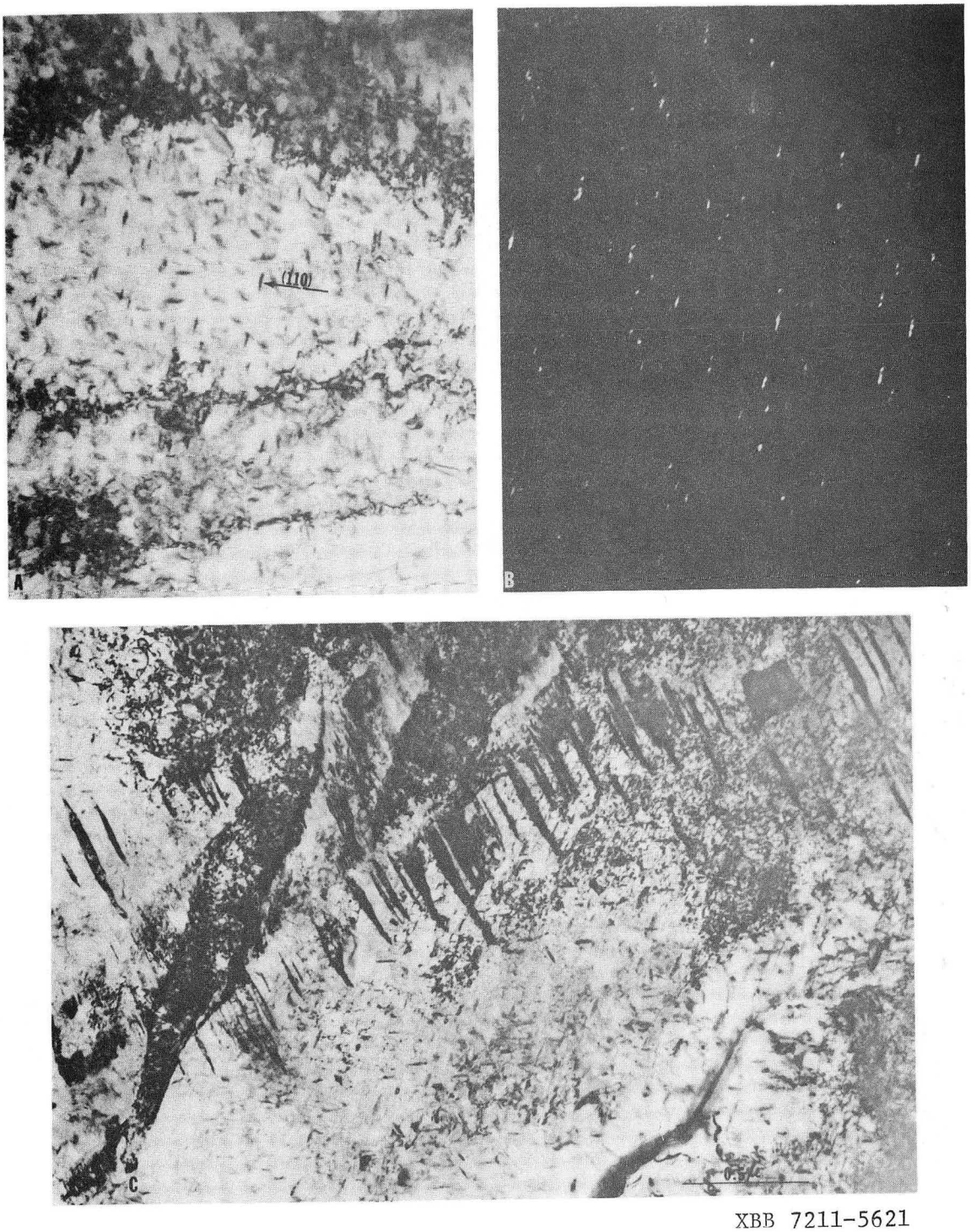


XBB 7211-5621

Fig. 3. As-quenched alloy 0417, showing bright field (a) and dark field (b) of autotempered carbides in a Widmanstatten pattern on $\{110\}_\alpha$ planes. (c) illustrates a single martensite plate with both autotempered carbides and transformation twins.

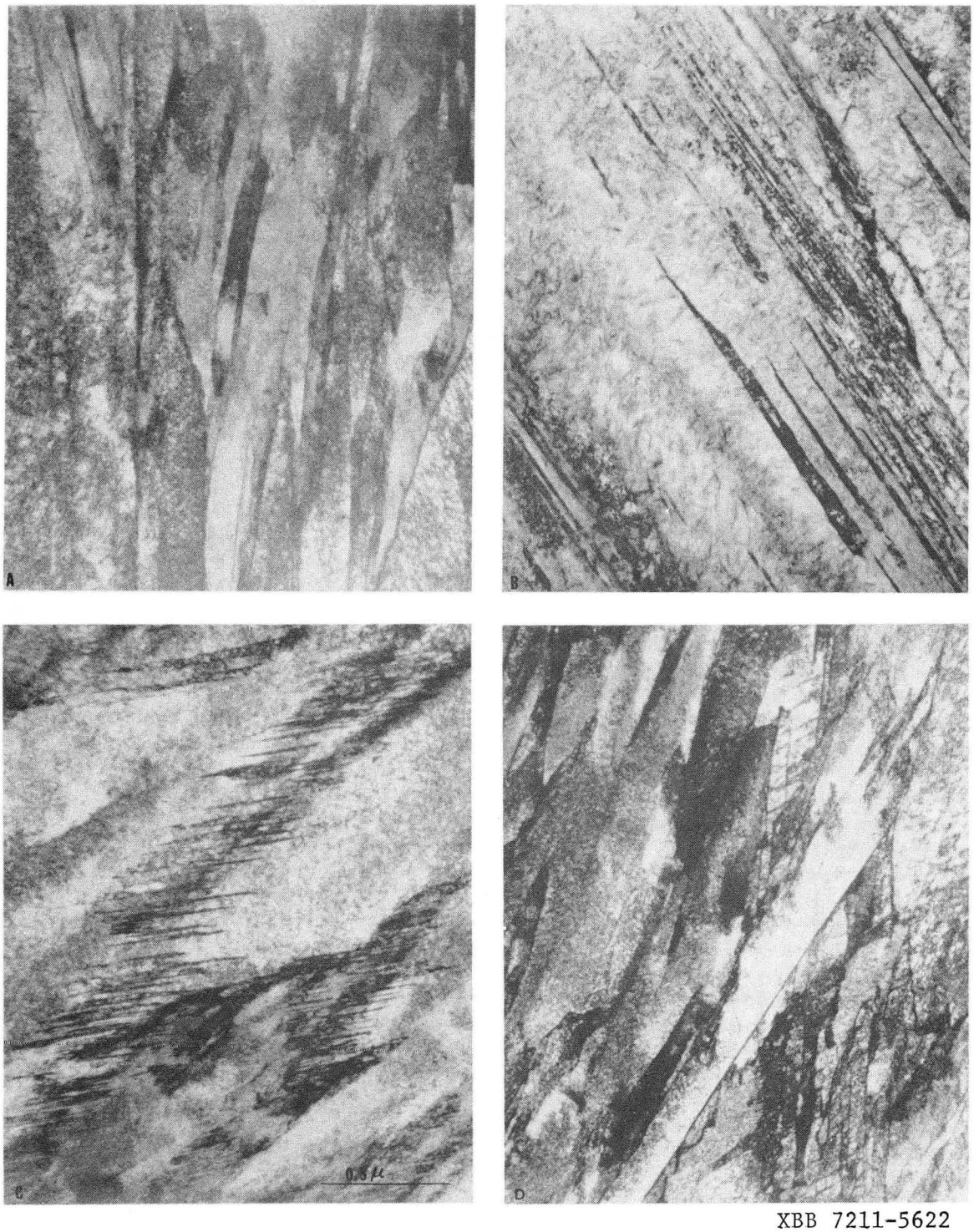


XBB 7211-5622

Fig. 4. Typical as-quenched microstructures of 0.35 wt.% C alloys. Alloy 0435 contains a mixed structure of dislocated laths (a) and twinned plates (b). Alloy 1235 also has a mixed structure, shown in (c) and (d), although the twin density in this alloy is much higher than that of alloy 0435.

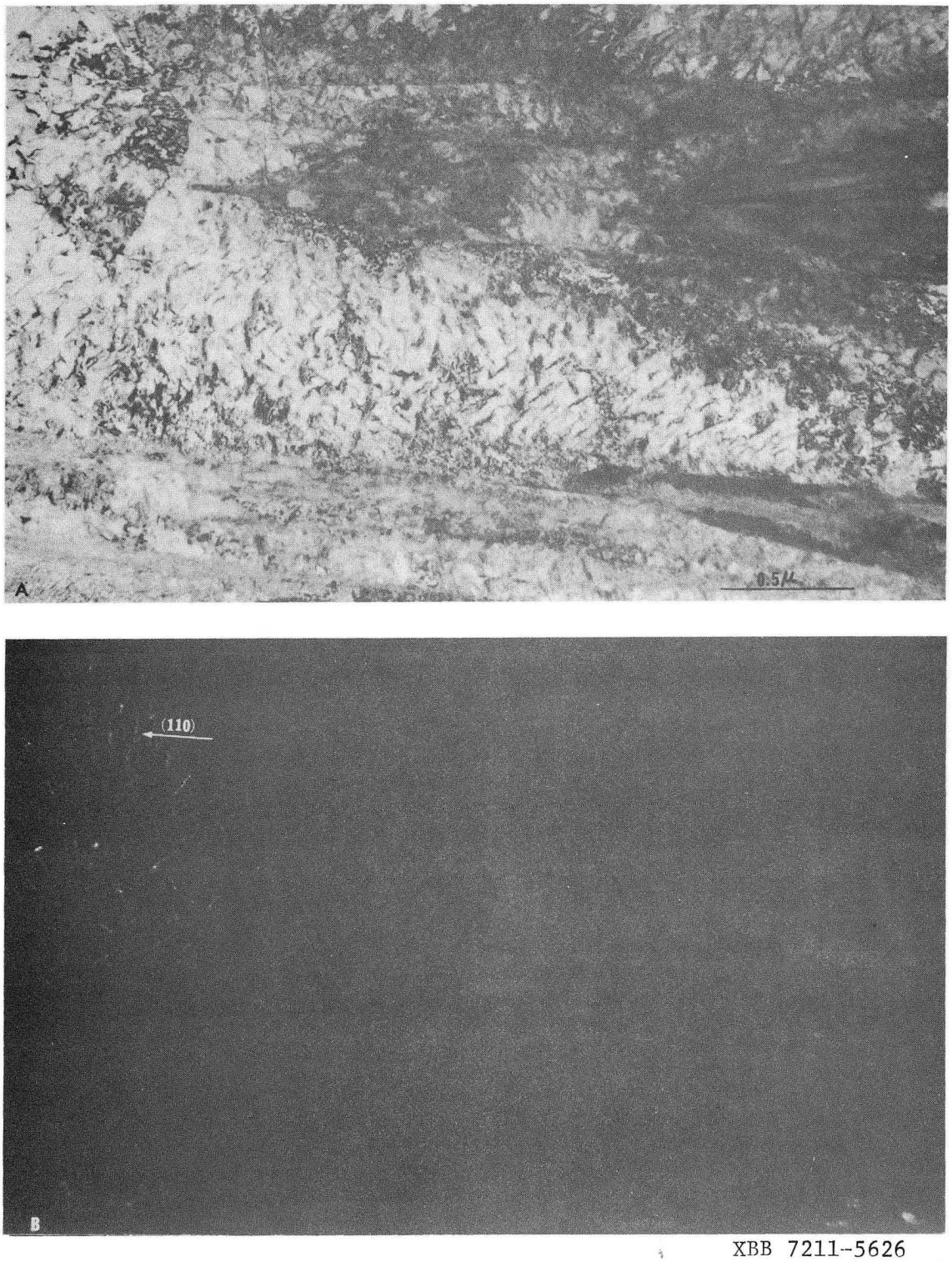


XBB 7211-5626

Fig. 5. Bright field (a) and dark field (b) of autotempered carbides in alloy 0435, showing the carbides in a Widmanstatten pattern on $\{110\}_\alpha$ planes.

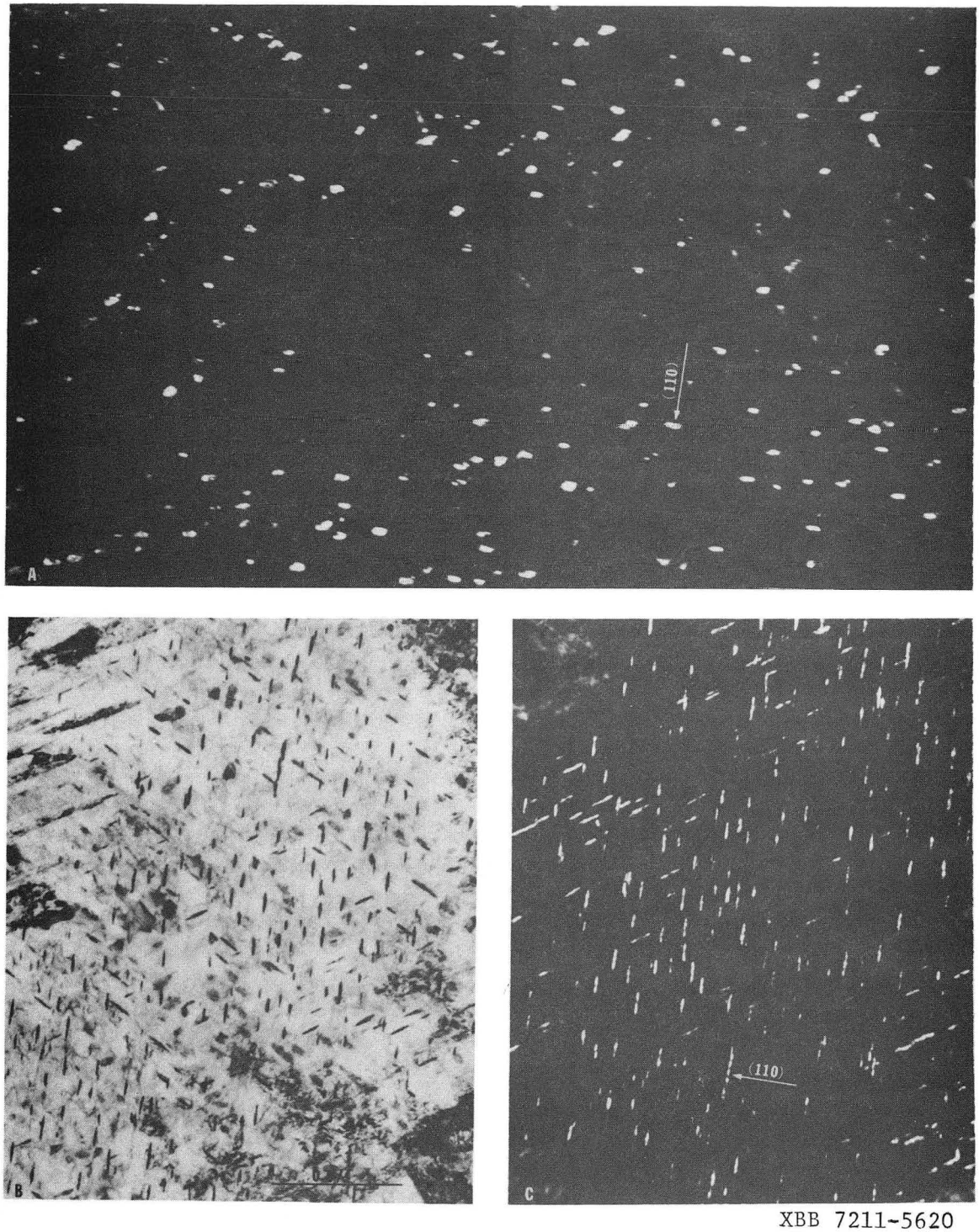


XBB 7211-5620

Fig. 6. Micrographs of 200°C tempered specimens. (b) and (c) show the Widmanstatten pattern of $Fe_3C$ in alloy 0817, which is typical of the 0.17 wt.% C alloys. The carbides formed at 200°C in alloy 0417 were coarser, as seen in (a).

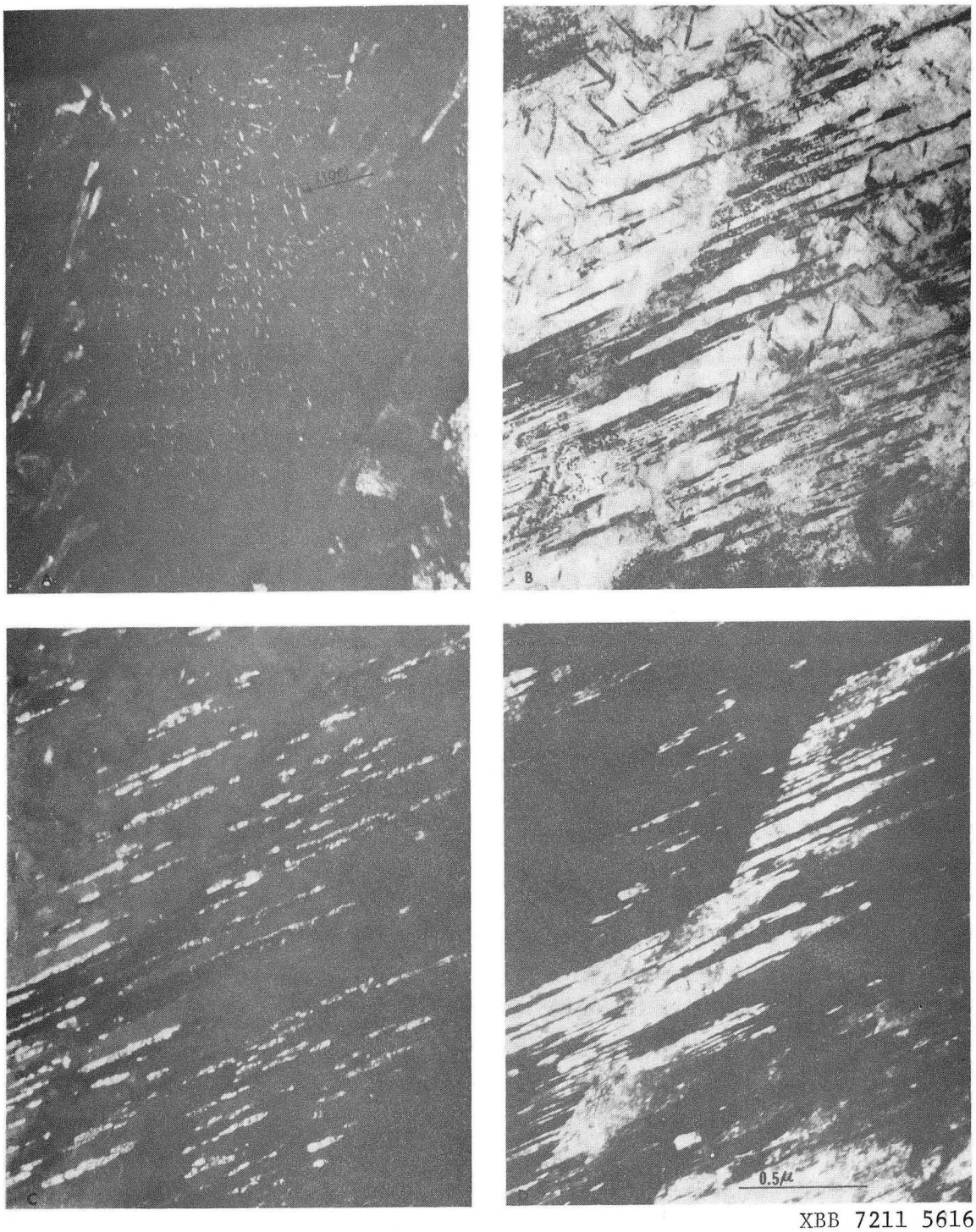


XBB 7211 5616

Fig. 7. Epsilon carbide formed in alloy 1235 at 200°C (a). The typical twin boundary carbide morphology of all the alloys tempered at 200 and 400°C is seen in (b) through (d). (b) is the bright field of a twinned region in alloy 0435, while (c) and (d) are the dark field images of the boundary carbides and the twins, respectively.

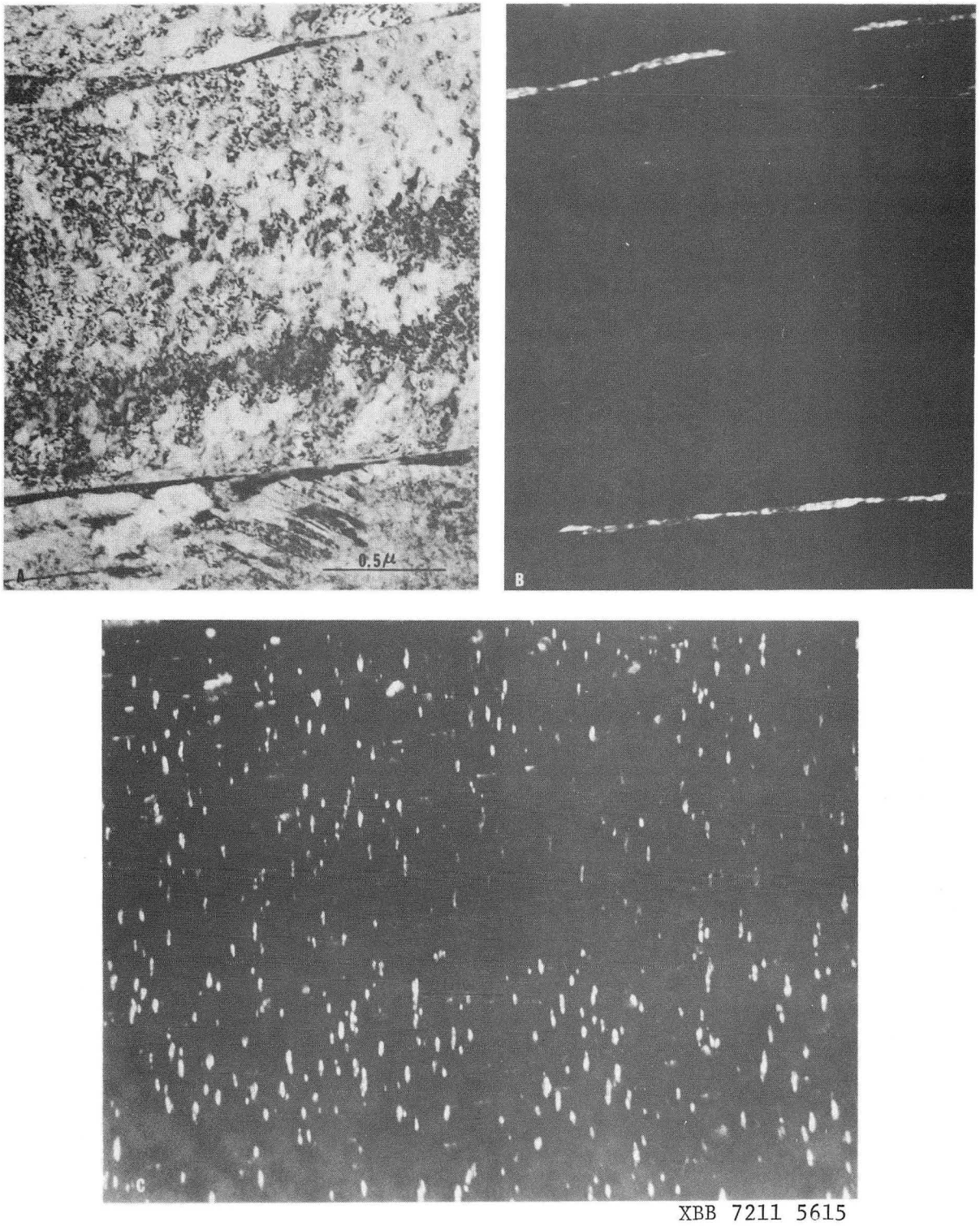


XBB 7211 5615

Fig. 8. Bright field (a) and dark field (b) of lath boundary carbides formed in alloy 0817 tempered at 400°C. The dark field (c) of matrix carbides in the same alloy show little coarsening at this temperature.

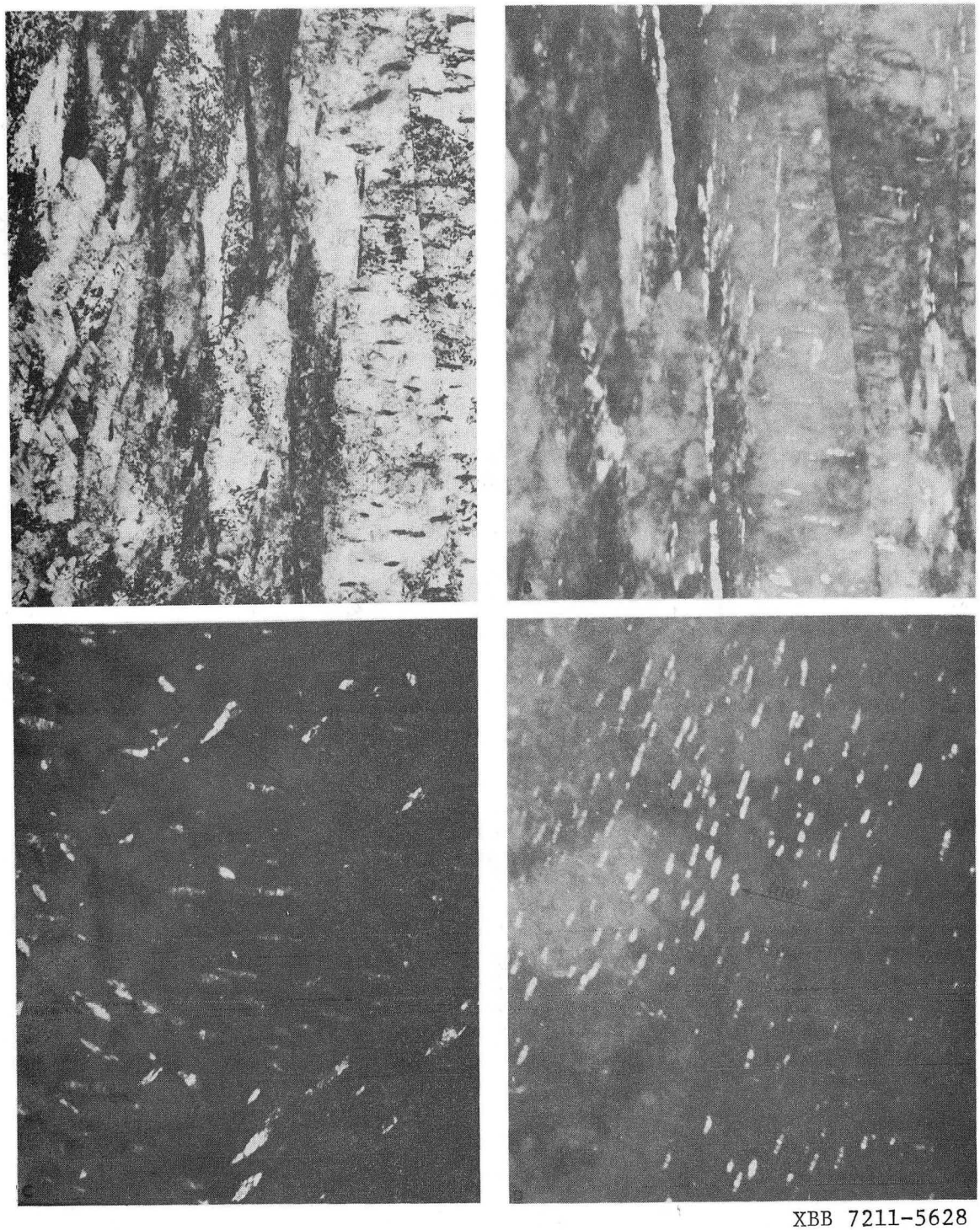

XBB 7211-5628

Fig. 9. Bright field (a) and dark field (b) of lath boundary carbides in alloy 0435 tempered at 400°C. (c) shows further coarsening of the matrix carbides in this alloy at 400°C, while the dark field image (d) of matrix carbides in alloy 1235 shows little carbides coarsening at 400°C.

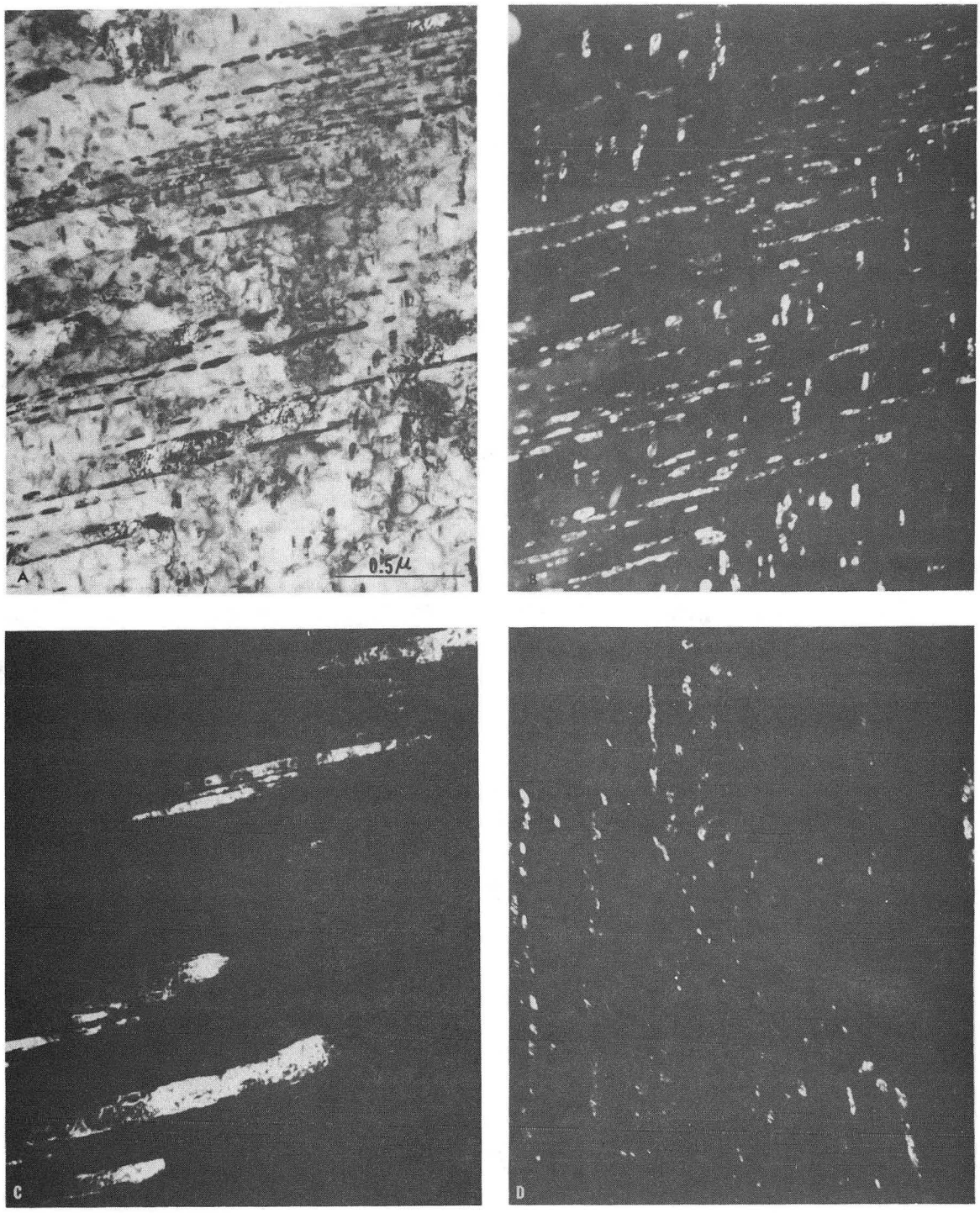


XBB 7211-5627

Fig. 10. Bright field (a), dark field of twin boundary and matrix carbides (b), dark field of twins (c), and dark field of lath boundary carbides (d) in alloy 0435 tempered at 600°C. Twin and lath boundary carbides are seen to be segmented and spheroidized.

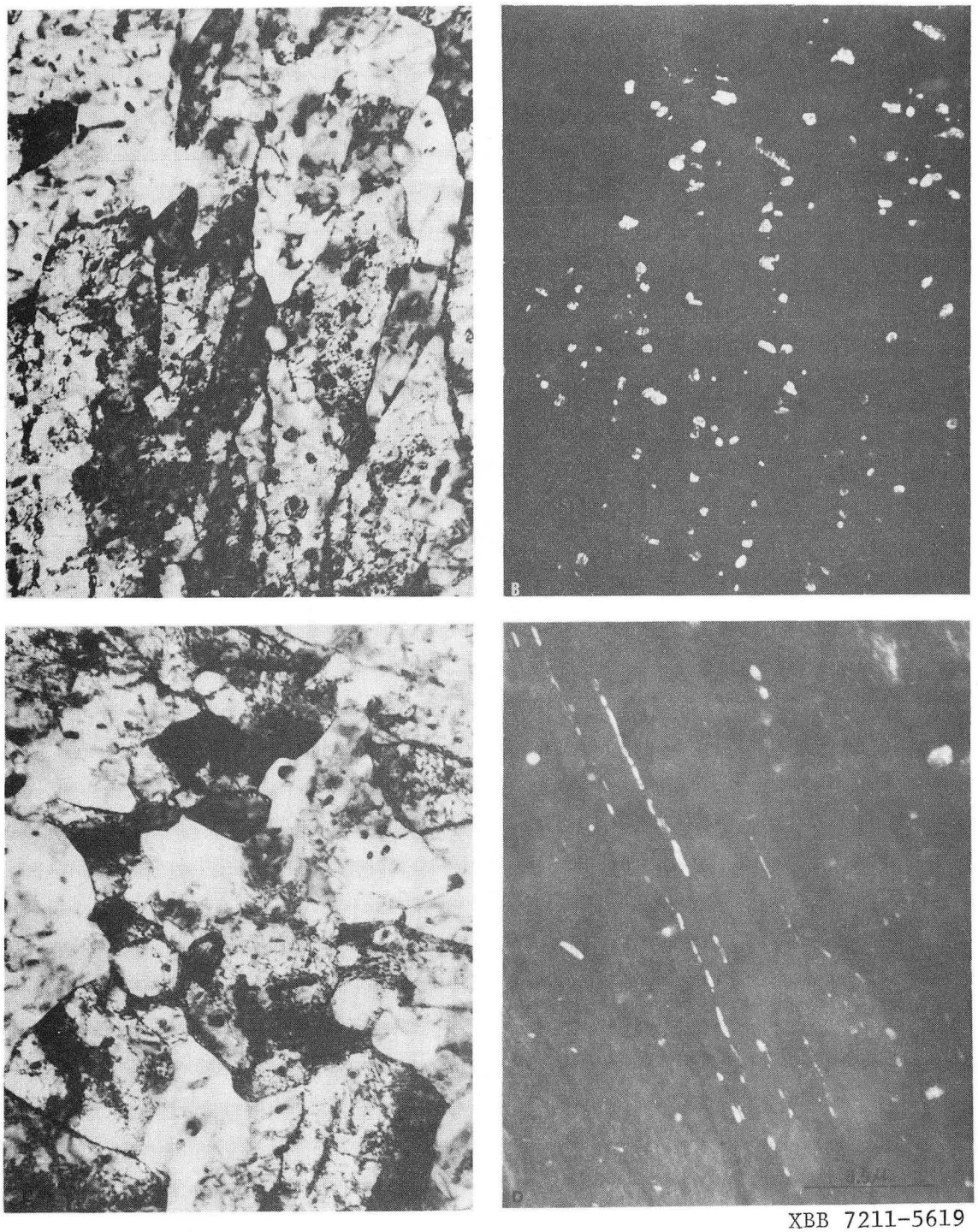

XBB 7211-5619

Fig. 11. Bright field (a) and dark field (b) of spheroidized matrix carbides in alloy 0435 tempered at 600°C. Recovery and recrystallization in this alloy at 600°C is evident in (c). (d) is the dark field image of segmented lath boundary carbides in alloy 0817 tempered at 600°C.

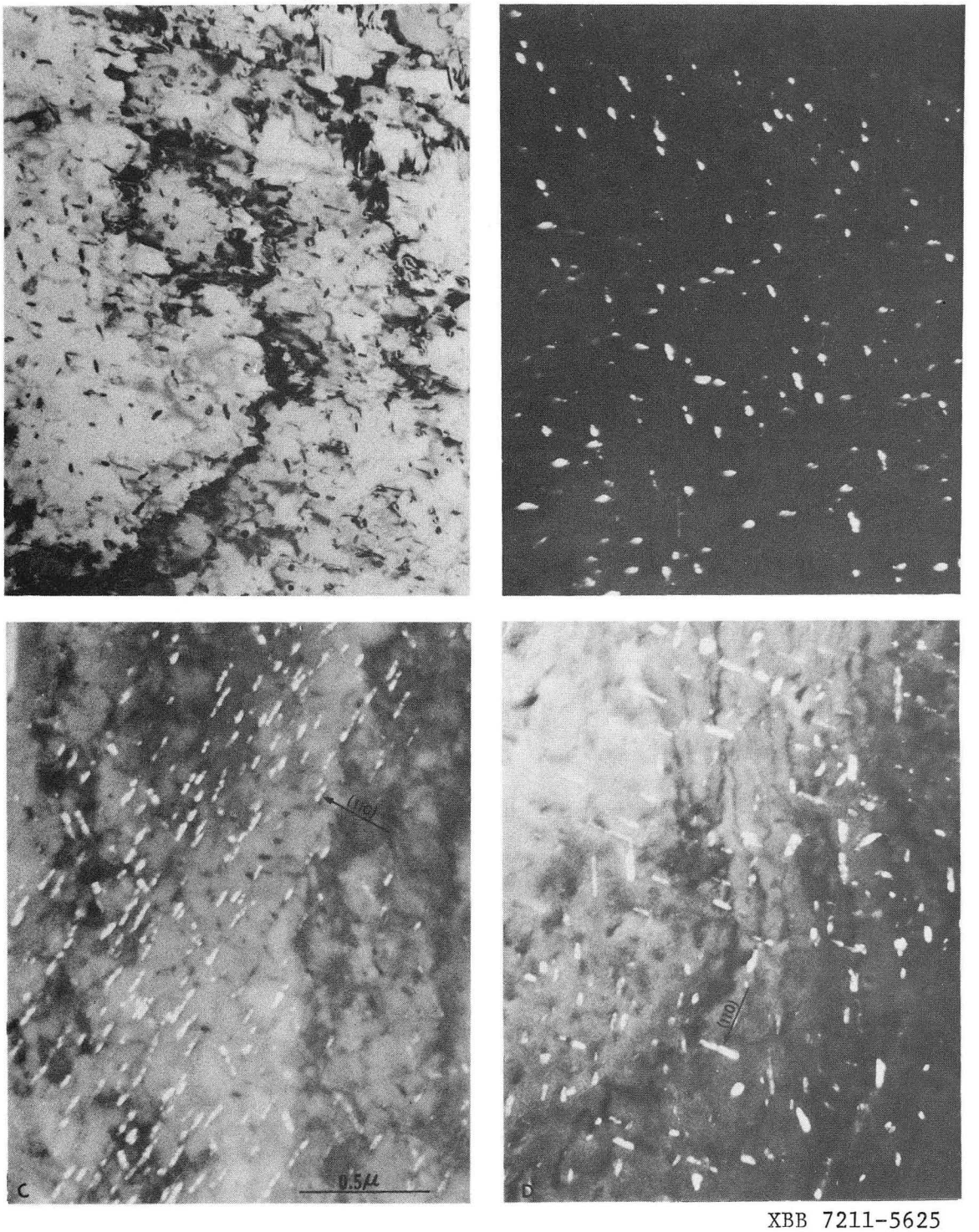


XBB 7211-5625

Fig. 12. Bright field (a) and dark field (b) of fine dispersion of $Cr_7C_3$ formed in alloy 0817 at 600°C. (c) and (d) show dark field images of the same type of alloy carbide distribution formed at 600°C in alloys 1235 and 0435, respectively.

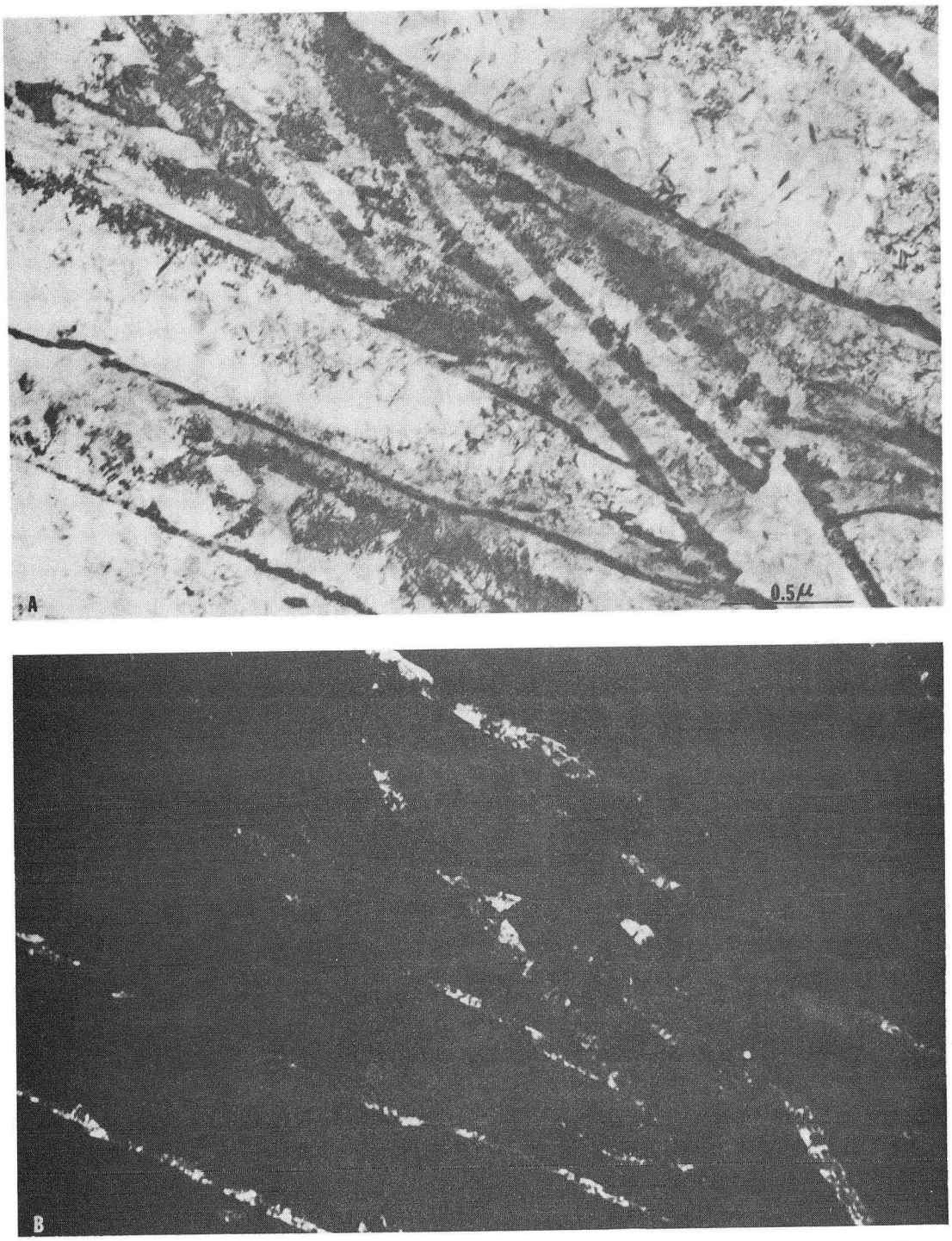


XBB 7211-5624

Fig. 13. Bright field image (a) of as-quenched alloy 0817, showing retained austenite films surrounding each martensite laths. The lath boundary films are illuminated in the dark field image (b) by using an FCC diffraction spot from the retained austenite.

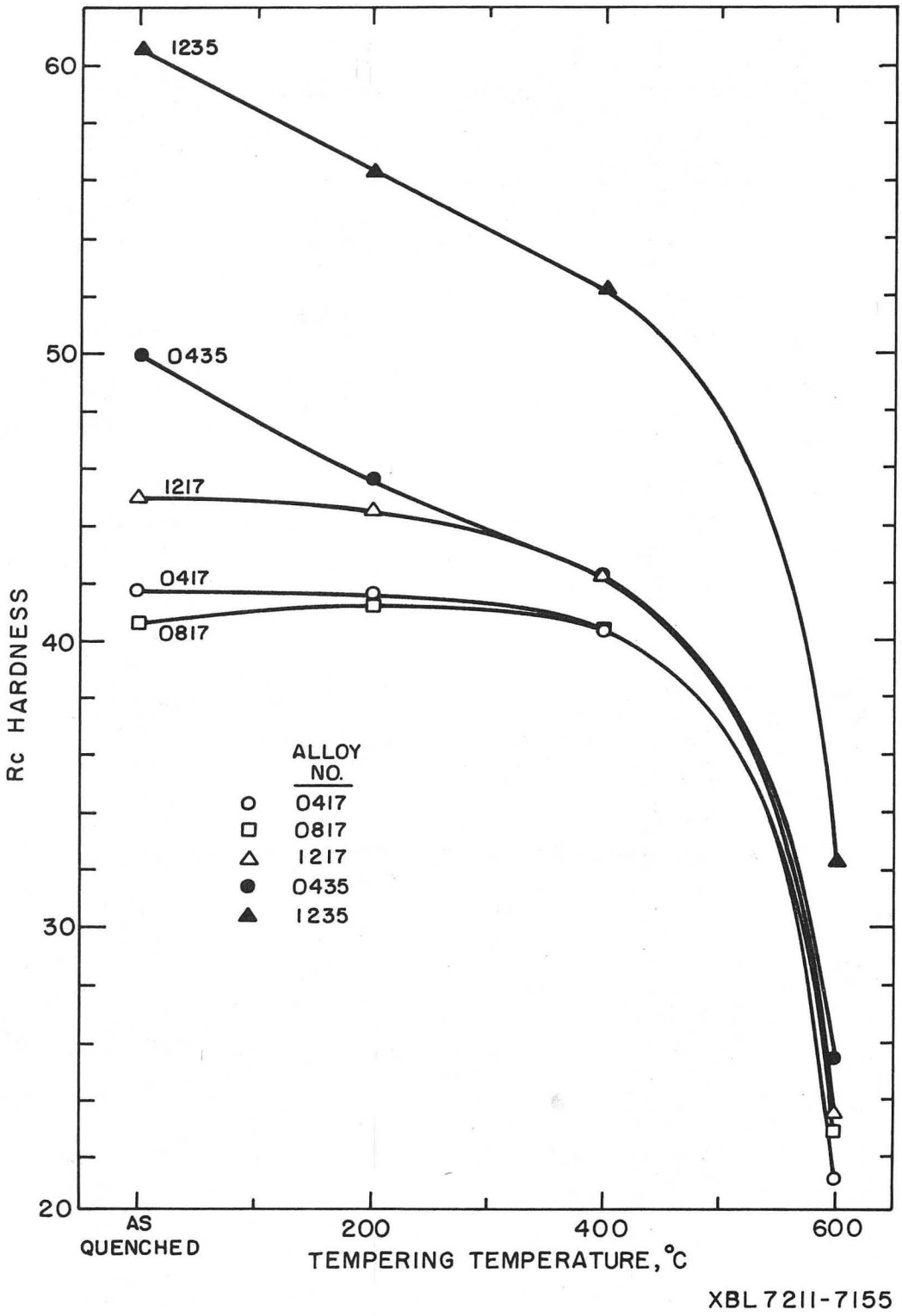


Fig. 14. $R_c$ hardness versus tempering temperature for all alloys.

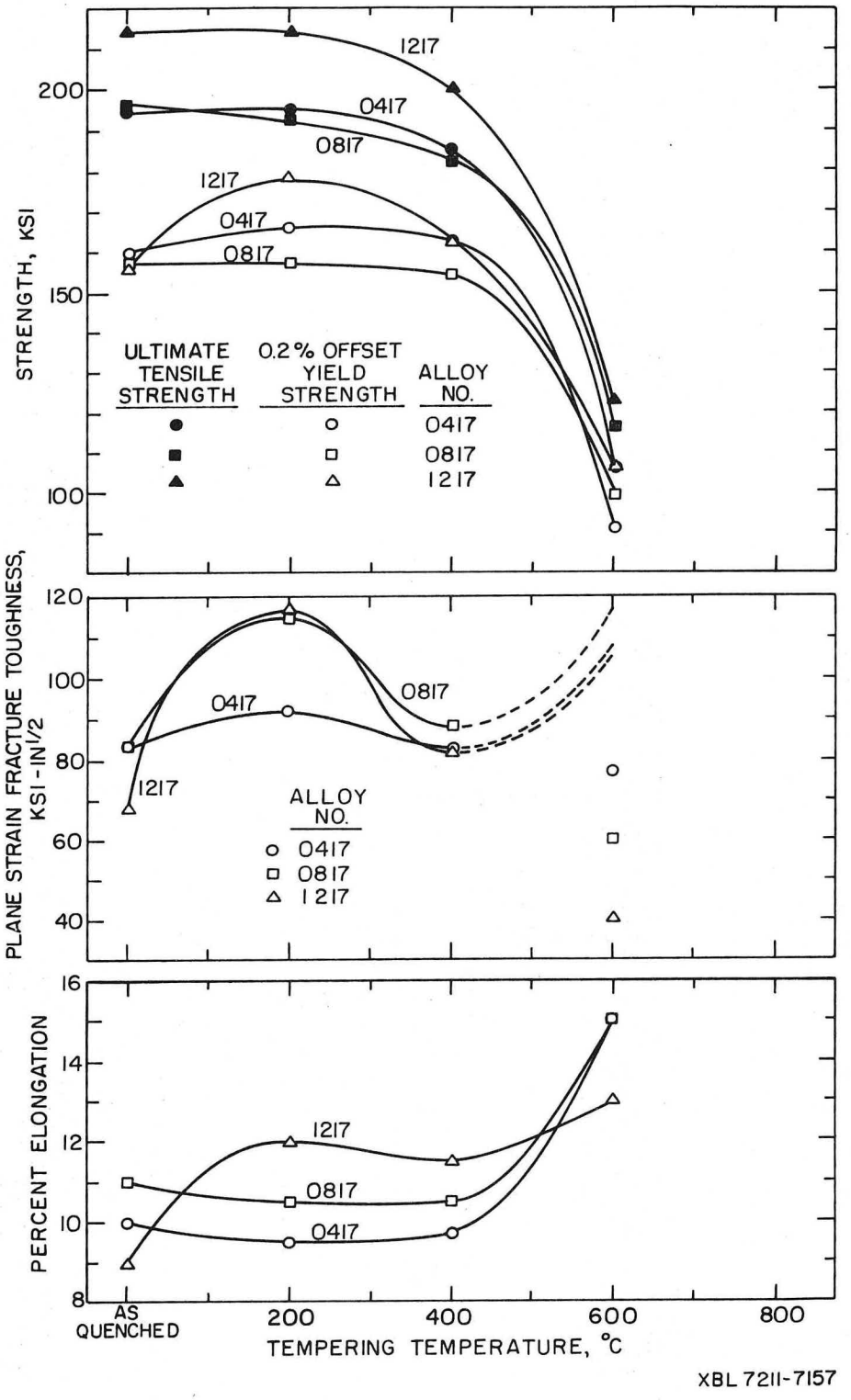


Fig. 15. Ultimate tensile strength, 0.3% offset yield strength, fracture toughness, and percent elongation of the 0.17 wt.% C alloys, as functions of tempering temperature.

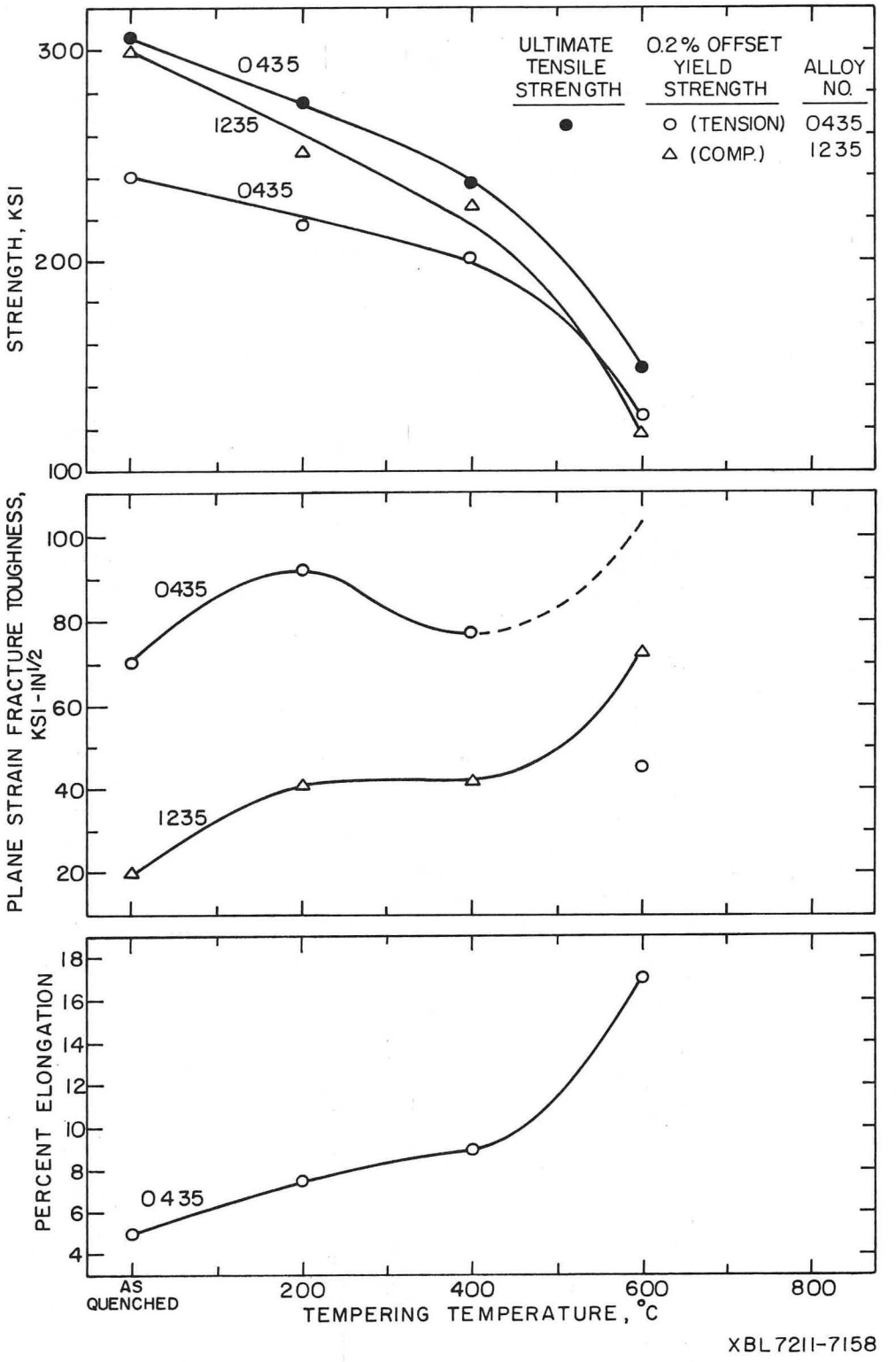


Fig. 16. Ultimate tensile strength, 0.2% offset yield strength, fracture toughness, and percent elongation of the 0.35 wt.% C alloys, as functions of tempering temperature.

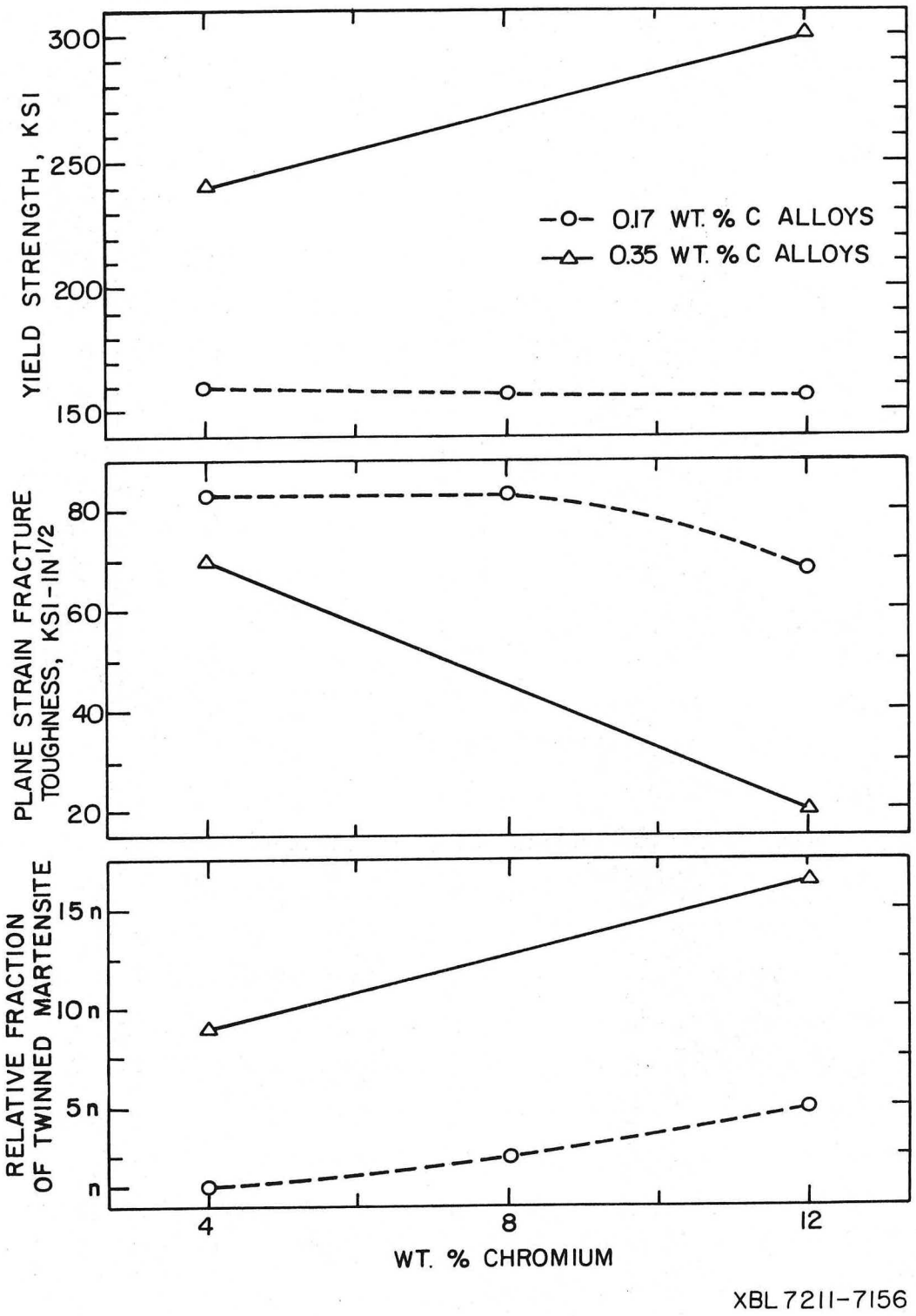


Fig. 17. As-quenched yield strength, fracture toughness, and relative fraction of twinned martensite of 0.17 and 0.35 wt.% C alloys, as functions of wt.% Cr.

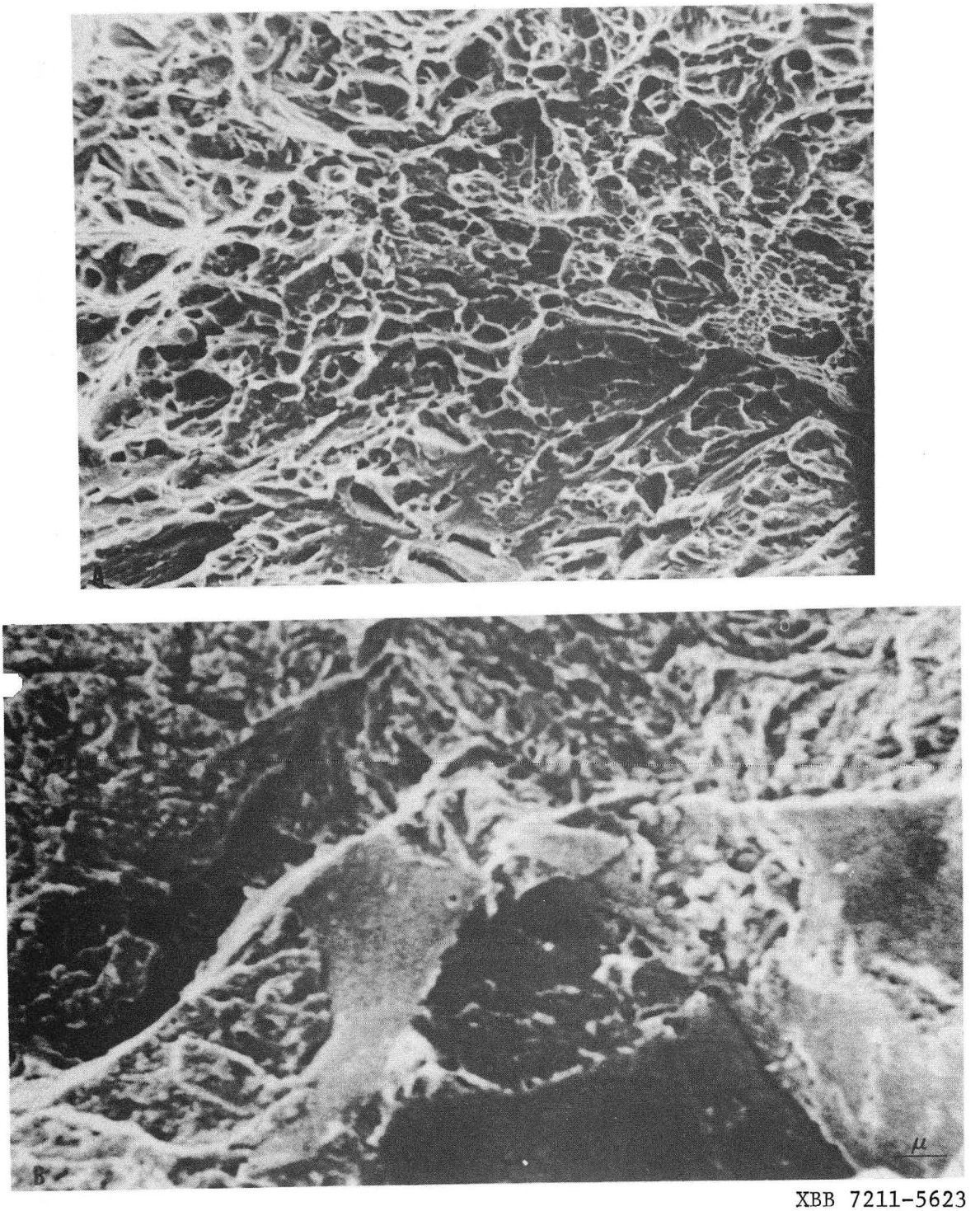


XBB 7211-5623

Fig. 18. Scanning electron fractographs of alloys 0435 (a) and 1235 (b).

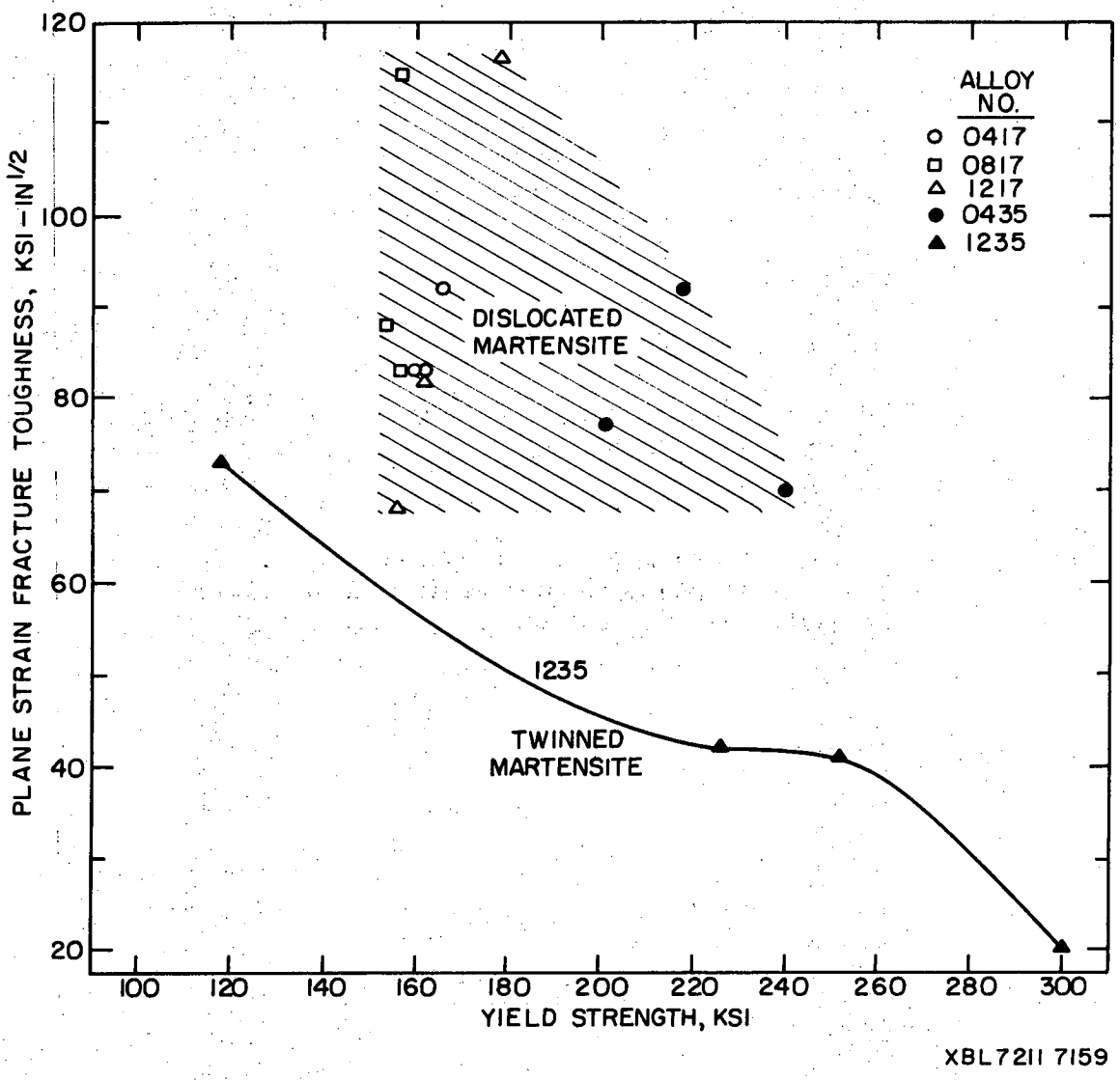


Fig. 19. Yield strength versus fracture toughness for all alloys under various tempering conditions, giving a strength/toughness comparison of dislocated and twinned martensites.

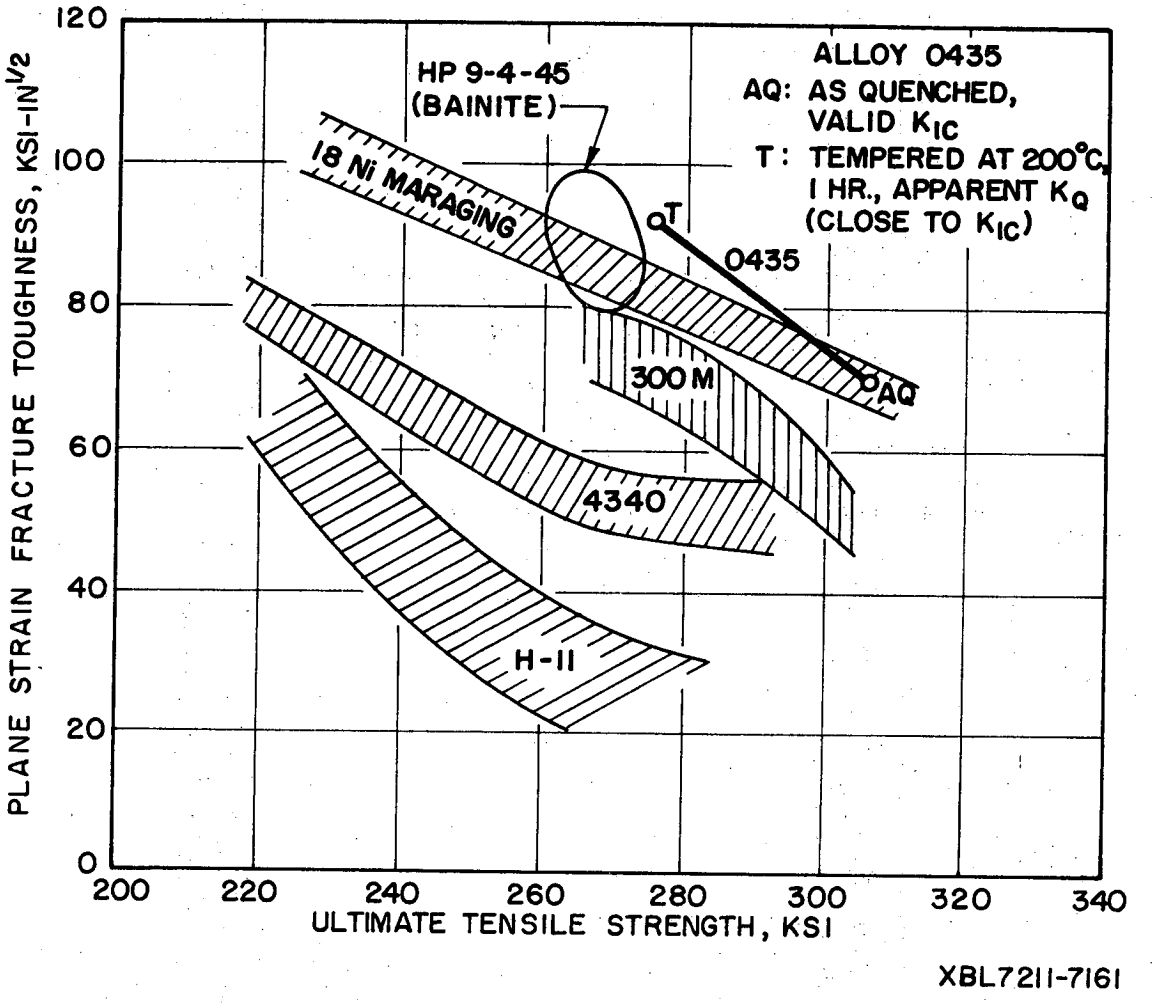


Fig. 20. Comparison of ultimate tensile strength and fracture toughness of alloy 0435 with the strength/toughness properties of several ultra-high-strength commercial steels. (See ref. 31)

*TECHNICAL INFORMATION DIVISION*
*LAWRENCE BERKELEY LABORATORY*
*UNIVERSITY OF CALIFORNIA*
*BERKELEY, CALIFORNIA 94720*